

Comparing Sequential Forecasters

Yo Joong Choe, Aaditya Ramdas

Department of Statistics and Data Science

Machine Learning Department

Carnegie Mellon University

yjchoe@cmu.edu, aramdas@cmu.edu

May 31, 2025

Abstract

Consider two or more forecasters, each making a sequence of predictions for different events over time. We ask a relatively basic question: how might we compare these forecasters, either online or post-hoc, while avoiding unverifiable assumptions on how the forecasts or outcomes were generated? This work presents a novel and rigorous answer to this question. We design a sequential inference procedure for estimating the time-varying difference in forecast quality as measured by a relatively large class of proper scoring rules (bounded scores with a linear equivalent). The resulting confidence intervals are nonasymptotically valid, and can be continuously monitored to yield statistically valid comparisons at arbitrary data-dependent stopping times (“anytime-valid”); this is enabled by adapting variance-adaptive *supermartingales, confidence sequences, and e-processes* to our setting. Motivated by Shafer and Vovk’s game-theoretic probability, our coverage guarantees are also distribution-free, in the sense that they make no distributional assumptions on the forecasts or outcomes. In contrast to a recent work by Henzi and Ziegel, our tools can sequentially test a *weak* null hypothesis about whether one forecaster outperforms another on average over time. We demonstrate their effectiveness by comparing forecasts on Major League Baseball (MLB) games and statistical postprocessing methods for ensemble weather forecasts.

Contents

1	Introduction	3
1.1	Related Work	5
2	Preliminaries	7
2.1	Martingales, Ville’s Inequality, and Confidence Sequences	7
2.2	Proper Scoring Rules	7
3	Confidence Sequences for Forecast Score Differentials	8
3.1	A Game-Theoretic Motivation	8
3.2	The Formal Setup	9
3.3	Scoring Rules with Linear Equivalents	11
3.4	Time-Uniform Confidence Sequences for Δ_t	12
3.4.1	Time-uniform Boundaries and Exponential Supermartingales	12
3.4.2	Warmup: Hoeffding-Style Confidence Sequences for Δ_t	12
3.4.3	Main Result: Empirical Bernstein Confidence Sequences for Δ_t	13
3.4.4	Choosing the Uniform Boundary u	14
3.5	e-Processes and Anytime-Valid p-Processes	16
4	Extensions	18
4.1	Comparing Probabilistic Forecasts on Categorical Outcomes	18
4.2	Comparing k -Step-Ahead Forecasts	20
4.3	Comparing Mean Forecasts on (Bounded) Continuous Outcomes	21
4.4	Winkler’s Normalized Score Differentials	22
5	Experiments	23
5.1	Simulated Experiments	23
5.2	Comparing Forecasters on Major League Baseball Games	29
5.3	Comparing Statistical Postprocessing Methods for Weather Forecasts	33
6	Conclusions	36
A	Tight Confidence Sequences via Uniform Boundaries	41
B	Proofs	41
B.1	Proof of Lemma 1	41
B.2	Proof of Theorem 2	41
B.3	Proof of Theorem 3	42
B.4	Proof of Lemma 3	43
B.5	Proof of Lemma 4	44
C	Computing the Gamma-Exponential Mixture	44
D	Comparing CS Widths on IID Means	46

Forecasts on Nationals Win	1	2	3	4	5	6	7
FiveThirtyEight ¹	37.9%	41.0%	52.7%	58.7%	37.3%	40.5%	48.5%
Vegas-Odds.com ²	34.9%	37.7%	41.0%	50.7%	33.7%	37.4%	43.1%
Adjusted Win Percentage	47.1%	47.4%	47.6%	47.4%	47.2%	47.0%	47.2%
K29 Defensive Forecast	50.0%	50.0%	50.9%	51.6%	50.7%	49.9%	49.1%
Constant Baseline	50.0%	50.0%	50.0%	50.0%	50.0%	50.0%	50.0%
Average Joe	40.0%	50.0%	60.0%	50.0%	30.0%	40.0%	50.0%
Nationals Fan	70.0%	70.0%	80.0%	70.0%	60.0%	60.0%	70.0%
Did the Nationals Win?	Yes	Yes	No	No	No	Yes	Yes

Table 1: Probability forecasts (%) on whether the Washington Nationals will win each game of the 2019 World Series. The first two forecasts are taken from publicly available websites online. The next three forecasts are baselines computed using the 10-year win/loss records (win probability is rescaled with the opponent’s win probability to sum to 1; see Section 5.2 for more details). The last two forecasts are imaginary (but not unrealistic) casual sports fans making their own forecasts using different heuristics. All forecasts are made prior to the beginning of each game. See Section 5.2 for more details on the forecasting methods and comparisons.

1 Introduction

Forecasts of future events and quantities are widely used in many domains, including meteorology, economics, epidemiology, elections, and sports. Often, we are given a set of forecasts made by different forecasters on a regularly occurring event, such as whether it will rain tomorrow and whether a sports team will win its next game. Other times, we are provided with forecasts on a future quantity across a time period, such as the number of weekly hospitalizations and deaths during a pandemic, the value of a stock market index, and the voter turnout.

Despite the popularity of forecasts across many domains, it is not obvious how we can evaluate and compare different forecasters on their predictive ability over time, as data is sequentially observed and the forecasts are subsequently updated. As an illustrative example, consider various game-by-game predictions made on the outcome of the 2019 World Series by real-world forecasters in Table 1. The outcome of a baseball game is clearly difficult to predict or model across time; furthermore, we also do not have full information on how the forecasts are generated. Had we been interested in determining which forecaster to trust going into the next game, how can we find out if one (if any) forecaster is better than another for predicting the winner of the next game? More generally, how do we determine that one forecaster is better than another at predicting the next outcome at *any* given time point, without having to make assumptions about how the reality behaves or how the forecasts are made?

In this work, we derive a statistically rigorous procedure for sequentially comparing the performances of such probability forecasts, using the powerful tool of *time-uniform confidence sequences (CS)* (Darling and Robbins, 1967; Lai, 1976b; Howard et al., 2021). CSs are sequences of confidence intervals that provide time-uniform and nonasymptotic coverage guarantees, enabling valid sequential inference at any stopping time for a time-varying parameter of interest, such as the difference in the average predictive performance up to time t . In particular, the coverage guarantees are valid both in the cases where inference is done sequen-

¹Source: <https://projects.fivethirtyeight.com/2019-mlb-predictions/games/>.

²Source: <https://sports-statistics.com/sports-data/mlb-historical-odds-scores-datasets/>.

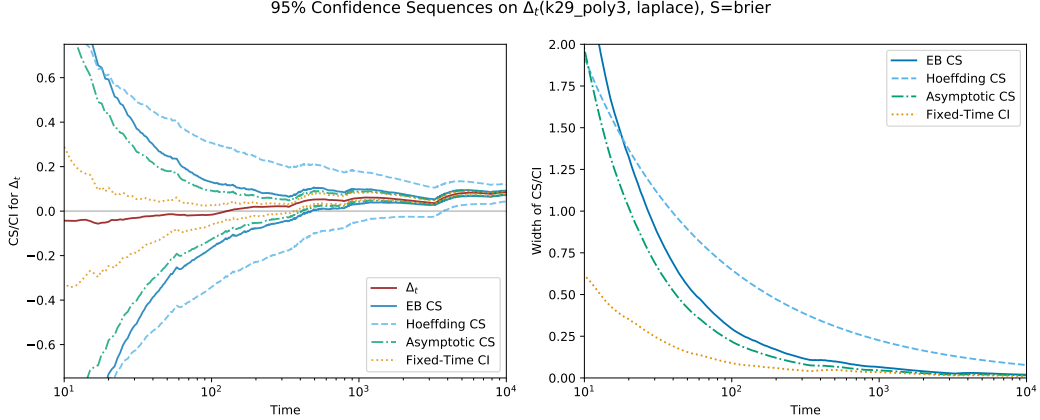


Figure 1: 95% empirical Bernstein CS (blue), Hoeffding-style CS (skyblue, dashed), asymptotic CS (green, dashdot), and fixed-time asymptotic CI (orange, dotted) for the average forecast score differentials Δ_t (left), along with their widths (right), between two forecasters on *synthetic* data with changepoints across $T = 10^4$ time steps. Scoring rule is the Brier score, and positive values of Δ_t indicate that the first forecaster is better than the second. All variants of CS, which we develop and discuss throughout the paper, cover Δ_t uniformly over all t , and the width of the EB CS approaches that of the asymptotic CS as time grows large. The fixed-time CI, which was developed by Lai et al. (2011), is tighter than the CSs, but it notably lacks a stopping time or a nonasymptotic guarantee. See Section 5 for further details.

tially after each outcome and in the case of post-hoc inference on the (sequentially) observed data. Figure 1 demonstrates how variants of CS we develop in our paper all uniformly cover the average forecast score differential Δ_t , which reflects the time-varying average difference in forecast quality measured using scoring rules (Gneiting and Raftery, 2007). Importantly, our empirical Bernstein (EB) CS, which has a non-asymptotic coverage guarantee at arbitrary stopping times is variance-adaptive, becomes nearly as tight as its fixed-time counterpart (a confidence interval without a stopping time guarantee; Lai et al. (2011)) as time grows large.

We motivate our derivation of confidence sequences by introducing a game-theoretic setup (Shafer and Vovk, 2019), in which two players play a sequential forecasting game on an outcome with an unknown parameter. This game highlights the sequential nature of the problem setting and the need for a time-uniform and distribution-free inference procedure. We then use the martingale theory of scoring rules with linear equivalents (Lai et al., 2011) to derive confidence sequences for the time-varying difference in average forecasting scores of the two forecasts. The resulting sequential inference procedure is time-uniform, nonasymptotic, and also distribution-free: we make virtually no assumptions on how the outcomes (and forecasts, in most cases) are actually generated.

The rest of the paper is organized as follows. After discussing related work in Section 1.1 and preliminaries in Section 2, in Section 3, we derive CSs for the time-varying average forecast score differentials between two probability forecasters on binary outcomes. In Section 3.5, we also derive *e-processes* and *anytime-valid p-processes* (Ramdas et al., 2020) as duals to our CSs that provide alternative sequential inference procedures for forecast comparison. In Section 4, we discuss several extensions of our CSs, including the cases of categorical and bounded continuous outcomes, k -step-ahead forecasts, and using normalized score differentials. In Section 5.1, we empirically validate our CSs and compare them against fixed-time and

Method & Key Result	Null (Implied or Stated)	ST	NA	DF
Diebold and Mariano (1995) $\sqrt{t}(\hat{\Delta}_t - \mu) \rightsquigarrow N(0, 2\pi f_d(0))$	$H_0 : \mathbb{E}[\hat{\delta}_t] = 0$	✗	✓/✗	✗ (stationarity)
Giacomini and White (2006) $T_m(\hat{\delta}_t) \rightsquigarrow \chi^2$ (m : window size)	$H_0 : \mathbb{E}[\hat{\delta}_t \mathcal{G}_{t-1}] = 0$	✗	✗	✗ (mixing)
Lai et al. (2011) $\sqrt{t}(\hat{\Delta}_t - \Delta_t)/s_t \rightsquigarrow N(0, 1)$	$H_0 : \mathbb{E}[\hat{\delta}_t \mathcal{G}_{t-1}] = 0$	✗	✗	✓
Ehm and Krüger (2018) $\frac{1}{\sqrt{t}} \sum_{i=1}^t \sigma_i \hat{\delta}_i(\theta) \rightsquigarrow N(0, \gamma(\theta)),$ ($\sigma_i = \pm 1$ w.p. $\frac{1}{2}$ each)	$H_0^w : \frac{1}{\sqrt{t}} \sum_{i=1}^t \mathbb{E}[\hat{\delta}_i(\theta) \mathcal{G}_{i-1}] = 0$ $H_0^s : \mathbb{E}[\hat{\delta}_i(\theta) \mathcal{G}_{i-1}] = 0, \forall i \leq t$	✗	✗	✗ (Lindeberg condition)
Henzi and Ziegel (2021) $E_t(\lambda) = \prod_{i=1}^t E_i(\lambda)$ is an NSM, where $E_i(\lambda) = 1 + \lambda \frac{\hat{\delta}_i}{ T(p_i, q_i) }$	$H_0^s : \mathbb{E}[\hat{\delta}_i(\theta) \mathcal{G}_{i-1}] \leq 0, \forall i \leq t$	✓	✓	✓
Ours $t(\hat{\Delta}_t - \Delta_t)$ is a sub- ψ process (upper-bounded by an NSM)	$H_0^w : \hat{\Delta}_t = \frac{1}{t} \sum_{i=1}^t \mathbb{E}[\hat{\delta}_i \mathcal{G}_{i-1}] \leq 0$	✓	✓	✓

Table 2: Comparison of popular inference methods for comparing probability forecasts. This table is meant to be a quick summary only; see referenced paper for the precise definitions, conditions, and guarantees for each method. $\hat{\delta}_t = S(p_t, y_t) - S(q_t, y_t)$ and $\hat{\Delta}_t = \frac{1}{t} \sum_{i=1}^t \hat{\delta}_i$ respectively refer to the pointwise and average score differential between forecasts p_t and q_t against the observation y_t at time t . **ST**: whether the method has a stopping time (or time-uniform) guarantee. **NA**: whether the method has a nonasymptotic guarantee. **DF**: whether the method has a distribution-free guarantee. The only methods that have all three guarantees are the last two, both of which involve nonnegative supermartingales (NSM).

asymptotic confidence intervals (CIs) on simulated data. Finally, in Sections 5.2 and 5.3 we apply our methods to real-world forecast comparison tasks, namely comparing game-by-game predictions in Major League Baseball (MLB) and comparing statistical postprocessing methods of ensemble weather forecasts.

1.1 Related Work

Evaluation and Comparison of Probability Forecasts. Evaluation of probability forecasts is a well-studied subject in the literature of statistics, economics, finance, and climatology, dating back to at least the works of Brier (1950); Good (1952); DeGroot and Fienberg (1983); Dawid (1984); Schervish (1989). Many of the work on scoring rules focus on the properties of forecasts induced by these scoring rules, namely calibration and the sharpness of probability forecasts. See Gneiting and Raftery (2007); Winkler et al. (1996); Gneiting et al. (2007) for in-depth reviews of the subject.

The problem of comparing probability forecasts while accounting for sampling uncertainty was first popularized by Diebold and Mariano (1995) (DM), who proposed tests of equal (historical) forecast accuracy using the differences in forecast errors. The DM test is based on the asymptotic normality of the average forecast score differentials, and it makes stationarity assumptions about the outcomes. Giacomini and White (2006) (GW) developed tests of *conditional* predictive accuracy given past information, allowing for the comparison of “which forecaster will be more accurate at the forecast target date” rather than which one performed better in the past. The GW test thus allows for nonstationarity, although its validity depends

on mixing and moment assumptions. Lai et al. (2011) presented a comprehensive overview of the aforementioned methods of forecast comparison and develops a martingale-based theory of scoring rules that have linear equivalents, such as the Brier score and the logarithmic score. They proved the asymptotic normality of both forecast scores and score differentials, leading to an asymptotic CI that we use as a point of comparison in our work. While the theory in Lai et al. (2011) is a building block for our work, the key difference is that we depart from the classical notions of asymptotic and fixed-size CIs, and instead develop asymptotic and nonasymptotic CSs that are valid at arbitrary stopping times, all while making virtually no assumption made on the data generating distribution.

Recently, Henzi and Ziegel (2021) constructed sequential tests of conditional forecast dominance based on e-processes (Grünwald et al., 2019; Shafer, 2021; Ramdas et al., 2021; Vovk and Wang, 2021). Despite being nonasymptotic, these test a “strong³ null” which states that one forecaster is better than the other at *every* point in time, which is something we anyway rarely believe apriori. Thus, rejecting the strong null only suggests that there exists *some* time point where the latter forecaster is better than the former, which may not come as a surprise. In contrast, our e-processes test whether one forecaster dominates the other *on average* over time (thus requiring consistent outperformance), and the CSs can even test such averaged nulls in a two-sided fashion (equivalently, it tests both one-sided nulls). We examine this distinction further in Sections 3.5 and 5.3.

Table 2 summarizes the aforementioned methods of forecast comparison. Note that we refer to the time-uniform guarantee as a stopping time guarantee, as the two conditions are in fact equivalent (Ramdas et al., 2020). See Section 3.5 for further details.

Time-Uniform Confidence Sequences. Confidence sequences (CSs) were developed by Robbins and coauthors (Darling and Robbins, 1967; Robbins, 1970; Robbins and Siegmund, 1970; Lai, 1976a). Recent renewed interest on CSs are partly due to best-arm identification in multi-armed bandits (Jamieson et al., 2014; Jamieson and Jain, 2018), where CSs are sometimes referred to as always-valid or anytime confidence intervals. CSs are also duals to sequential hypothesis tests, analogous to confidence intervals being dual to fixed-time hypothesis tests, and one can further derive a sequence of e-processes and anytime-valid p-values given the CSs (more precisely, its underlying exponential process) (Ramdas et al., 2021). In Section 3.5, we make this connection explicit and discuss how our approach also leads to anytime-valid p-processes (Johari et al., 2015) for weak nulls.

The recent work by Howard et al. (2021) is of particular importance in our work, as it develops a class of tight confidence sequences that are uniformly valid over time with nonparametric assumptions and has widths that shrink to zero. This work and its underlying technique of nonnegative supermartingales (NSMs) (Howard et al., 2020; Ville, 1939) has led to several interesting results, including state-of-the-art concentration inequalities for mean estimation (Waudby-Smith and Ramdas, 2020), doubly robust sequential causal inference (Waudby-Smith et al., 2021), and off-policy evaluation for contextual bandits (Karampatziakis et al., 2021). Our work makes the connection between the empirical Bernstein (EB) CSs derived in Howard et al. (2021) and the martingale property of forecast score differentials (Lai et al., 2011), leading to a novel sequential inference procedure for anytime-valid forecast comparison.

³This distinction of strong and weak nulls come from the discussion of randomization experiments in the causal inference literature; see, e.g., Lehmann (1975); Rosenbaum (1995); Wu and Ding (2020). Within the context of sequential forecast comparison, Ehm and Krüger (2018) makes the distinction between tests of average and step-by-step conditional predictive ability, which mirrors that of weak and strong nulls.

2 Preliminaries

2.1 Martingales, Ville's Inequality, and Confidence Sequences

Let $(\Omega, \mathcal{G}, \mathbb{P})$ be a probability space with filtration $(\mathcal{G}_t)_{t=1}^\infty$, with each \mathcal{G}_t representing the accumulated information up to time $t = 1, 2, \dots$. A sequence of random variables $(X_t)_{t=1}^\infty$ is *adapted* to $(\mathcal{G}_t)_{t=1}^\infty$ if $X_t \in \mathcal{G}_t$ for each t and *predictable* if $X_{t+1} \in \mathcal{G}_t$ for each t . A sequence $(X_t)_{t=1}^\infty$ adapted to $(\mathcal{G}_t)_{t=1}^\infty$ is a *supermartingale* if $\mathbb{E}[|X_t|] < \infty$ and $\mathbb{E}[X_{t+1} | \mathcal{G}_t] \leq X_t$ for each t . $(X_t)_{t=1}^\infty$ is a *submartingale* if $(-X_t)_{t=1}^\infty$ is a supermartingale, and it is a *martingale* if it is both a supermartingale and a submartingale. Moreover, a sequence $(D_t)_{t=1}^\infty$ adapted to $(\mathcal{G}_t)_{t=1}^\infty$ is a *martingale difference sequence* if $\mathbb{E}[|D_t|] < \infty$ and $\mathbb{E}[D_t | \mathcal{G}_{t-1}] = 0$ for each t .

If $(X_t)_{t=1}^\infty$ is a *nonnegative supermartingale* with respect to $(\mathcal{G}_t)_{t=1}^\infty$ and $X_1 = 1$, then Ville's inequality (Ville, 1939) states that, for any $\alpha \in (0, 1)$,

$$\mathbb{P}(\exists t \geq 1 : X_t > 1/\alpha) \leq \alpha. \quad (1)$$

Ville's inequality is the primary tool for constructing confidence sequences, as illustrated in, e.g., Howard et al. (2021); in fact, it is the only admissible way to construct them (Ramdas et al., 2020). Given $\alpha \in (0, 1)$, a $(1 - \alpha)$ -level *confidence sequence* (CS) for a time-varying sequence of target parameters $(\theta_t)_{t=1}^\infty$ is a sequence of confidence intervals (CIs) $(C_t)_{t=1}^\infty$ such that

$$\mathbb{P}(\exists t \geq 1 : \theta_t \notin C_t) \leq \alpha, \text{ or equivalently, } \mathbb{P}(\forall t \geq 1 : \theta_t \in C_t) \geq 1 - \alpha. \quad (2)$$

This coverage guarantee over all times is sometimes referred to as being *time-uniform* or *anytime-valid*. In particular, the guarantee remains valid at arbitrary stopping times and without a prespecified sample size, so that collecting additional data over time does not invalidate it. This crucially differentiates a CS from a fixed-time CI C_n , which only has the following (much) weaker guarantee:

$$\forall n \geq 1, \mathbb{P}(\theta_n \notin C_n) \leq \alpha, \text{ or equivalently, } \forall n \geq 1, \mathbb{P}(\theta_n \in C_n) \geq 1 - \alpha. \quad (3)$$

In short, CSs are much more appropriate tools than CIs for sequential inference.

2.2 Proper Scoring Rules

Given a probability forecast $p \in [0, 1]$ for the binary outcome $y \in \{0, 1\}$, whose (unknown) mean is $r \in [0, 1]$, we define *scoring rule*⁴ $S : [0, 1] \times [0, 1] \rightarrow \mathbb{R}$ as any function that quantifies the quality of the forecast p compared against r (or y , when r is unknown). Following Gneiting and Raftery (2007), we take scoring rules to be *positively oriented*, in the sense that larger scores indicate better forecasts.

A scoring rule is *proper*⁵ if $S(r, r) \geq S(p, r)$ for any $p, r \in [0, 1]$, and it is *strictly proper* when $S(r, r) = S(p, r)$ if and only if $p = r$. Proper scoring rules are typically considered as the primary means of evaluating probabilistic forecasts, as they assess both calibration and sharpness of the forecasts (Winkler et al., 1996; Gneiting et al., 2007), while encouraging

⁴The literature on scoring rules is extensive and encompasses forecasts in the form of general probability distributions. While we start our discussion with probability forecasts on binary outcomes, we also discuss the cases of categorical, vector-valued, and continuous outcomes in Section 4. See, e.g., Winkler et al. (1996); Gneiting and Raftery (2007); Gneiting and Katzfuss (2014) for more comprehensive overviews.

⁵In the case of probability forecasts, proper scoring rules coincide with consistent scoring functions for the mean (Gneiting, 2011; Gneiting and Katzfuss, 2014). Proper scoring rules can be more generally defined for probabilistic (distributional) forecasts for non-discrete outcomes, which are beyond the scope of our work.

forecasters to be honest (Garthwaite et al., 2005), in the sense that they have no reason to report forecasts that are more optimistic/pessimistic than their actual beliefs about the eventual outcome.

Classical examples of proper scoring rules for binary outcomes include the following:

- The Brier score or the quadratic score (Brier, 1950):

$$S(p, r) = -(p - r)^2.$$

- The spherical score (Good, 1971):

$$S(p, r) = \frac{pr + (1 - p)(1 - r)}{\sqrt{p^2 + (1 - p)^2}}.$$

- The logarithmic score (Good, 1952):

$$S(p, r) = r \log(p) + (1 - r) \log(1 - p).$$

- The zero-one score or the success rate:

$$S(p, r) = r \mathbf{1}(p \geq 0.5) + (1 - r) \mathbf{1}(p < 0.5).$$

The Brier, spherical, and logarithmic scores are examples of strictly proper scoring rules, while the zero-one score is an example of a proper but not strictly proper scoring rule. It is important to note that, when comparing two forecasts p and q against r , we have that $S(p, r) - S(q, r)$ is linear in r for all of these examples. Also note that all of the examples except the logarithmic score are bounded for $p, r \in [0, 1]$.

3 Confidence Sequences for Forecast Score Differentials

In this section, we derive confidence sequences for the time-varying difference in the quality of forecasts, as measured by a proper scoring rule. Our intuition comes from the extensive literature on evaluating and comparing probability forecasts via scoring rules (Winkler et al., 1996; Gneiting and Raftery, 2007; DeGroot and Fienberg, 1983; Schervish, 1989; Lai et al., 2011), combined with the powerful tool of time-uniform confidence sequences (Darling and Robbins, 1967; Howard et al., 2021). Our discussion in this section focuses on the case of comparing probability forecasts on sequences of binary outcomes; we discuss extensions to categorical outcomes, bounded continuous outcomes, and k -step-ahead forecasts in Section 4.

3.1 A Game-Theoretic Motivation

The intuition behind our CS for forecast score differentials comes from the game-theoretic statistical framework (Shafer and Vovk, 2019). Consider a forecasting game where two players make probability forecasts on an event that happens over time (e.g., whether it will rain on each day, whether a sports team will win its game each week, and more) and an unknown player named reality generates the sequence of binary outcomes that the forecasters are trying to predict.

Let $t = 1, 2, \dots$ denote each round of the game. Though not required, we can also optionally allow having any historical data $y_{-(H-1)}, \dots, y_{-1}, y_0$ for any window size $H \geq 0$. The forecasting game can be formulated as follows:

Game 1 (Comparing Sequential Probability Forecasts). *For rounds $t = 1, 2, \dots$:*

1. *Forecasters 1 and 2 make their probability forecasts, $p_t, q_t \in [0, 1]$ respectively.* The order in which the forecasters make their forecasts is not specified.
2. *Reality chooses $r_t \in [0, 1]$.* r_t is not revealed to the forecasters.
3. *$y_t \sim \text{Bernoulli}(r_t)$ is sampled and revealed to the forecasters.*

At each round t , forecasters can make their probability forecasts using any information available to them. This includes historical and previous outcomes $y_{-(H-1)}, \dots, y_0, y_1, \dots, y_{t-1}$, any of the previous forecasts made, $p_1, \dots, p_{t-1}, q_1, \dots, q_{t-1}$, as well as any other side information available to either forecaster. They cannot, however, make their predictions using any of r_1, \dots, r_t 's (or information from the future). Reality, on the other hand, can essentially choose r_t “however they want,” and they can even choose r_t after seeing p_t or q_t , although in practice the reality is not usually influenced by the forecasters. Our goal, as the statistician, is then to rigorously compare the predictive performance of the two forecasters according to a chosen scoring rule, without making any assumptions on the behavior of any player involved.⁶

There are several important benefits to deriving a valid sequential inference approach for comparing the two forecasters over time in Game 1. First, there are no assumptions of stationarity or conditional independence on the sequence $(r_t)_{t=1}^\infty$ that generates the binary outcomes $(y_t)_{t=1}^\infty$, meaning that the approach would be valid for *any* sequence of binary outcomes. Also, there are no assumptions made on how the individual forecasts $(p_t)_{t=1}^\infty$ and $(q_t)_{t=1}^\infty$ are made, other than the fact that they do not depend on the unknown sequence $(r_t)_{t=1}^\infty$ that generates the outcomes $(y_t)_{t=1}^\infty$. Finally, the game is naturally sequential, such that the most useful comparison of the two forecasters would be to consider their performance over time. In particular, the comparison should be valid *at any given time*, as opposed to having a fixed sample size, and reflect which one is *usually*, as opposed to absolutely or always, better. The CSs we derive in the forthcoming sections will take advantage of all of these benefits, contrasting with existing approaches that fall short on one or more of these aspects.

3.2 The Formal Setup

We now formalize Game 1 in the context of comparing the two probability forecasters over time. Let $(p_t)_{t=1}^\infty$ and $(q_t)_{t=1}^\infty$ be any pair of sequences of probability forecasts, each taking a value in $[0, 1]$, for a sequence of binary outcomes $(y_t)_{t=1}^\infty$. (We discuss extensions to bounded real-valued outcomes and vector-valued outcomes in Section 4.) As illustrated in Game 1, the forecasts p_t and q_t at time t can depend on *any* available information before observing y_t , including previous outcomes $y_{-H}, \dots, y_0, y_1, \dots, y_{t-1}$, (own or others') forecasts $p_1, q_1, \dots, p_{t-1}, q_{t-1}$, as well as any other external information available to the forecasters. We now formalize Game 1 in a measure-theoretic sense by specifying each player's filtration, i.e., a sequence of “information sets” available to the player.

Forecasters' Filtration $(\mathcal{F}_t)_{t=1}^\infty$. We represent any information available to the forecasters before making their predictions at time t collectively as \mathcal{F}_{t-1} — in other words, $(\mathcal{F}_t)_{t=1}^\infty$ is a filtration to which $(p_t)_{t=1}^\infty$ and $(q_t)_{t=1}^\infty$ are predictable. For example, when predicting the

⁶Specifically, we do not consider mechanism design issues or strategic issues here, as we are primarily concerned with how to make the sequential comparison given a scoring rule and a pair of (arbitrary) forecasters. A separate line of work considers these important, but orthogonal, issues.

outcome of the next baseball game, the forecasters' filtration may include not only all of previous games' results but also any side information that either forecaster may have, such as which players are starting the game and whether there are injuries. The setup also allows for the case where two forecasters have different side information, as our results are completely agnostic to such details, but we use one filtration for the forecasters for the sake of clarity. Note that the framework allows for k -step ahead forecasts $(p_{t+k})_{t=1}^{\infty}$ and $(q_{t+k})_{t=1}^{\infty}$ for any $k \geq 1$, which are also predictable w.r.t. $(\mathcal{F}_t)_{t=1}^{\infty}$. Aside from requiring that the forecasts cannot depend on the future, we put no restrictions on how these forecasts are generated, and we only evaluate forecasters based on the forecasts they did make, as opposed to forecasts they would have made had previous outcomes been different (Dawid, 1984).

Reality's Filtration $(\mathcal{R}_t)_{t=1}^{\infty}$. Analogous to the forecasters' filtration, we define $(\mathcal{R}_t)_{t=1}^{\infty}$ as the filtration to which the reality sequence $(r_t)_{t=1}^{\infty}$ is predictable. The definition of $(\mathcal{R}_t)_{t=1}^{\infty}$ is completely general, in the sense that it represents whatever information set with which reality chooses its sequence $(r_t)_{t=1}^{\infty}$. Note that, since $(r_t)_{t=1}^{\infty}$ is predictable w.r.t. $(\mathcal{R}_t)_{t=1}^{\infty}$ and $y_t \sim \text{Bernoulli}(r_t)$, we have

$$\mathbb{E}[y_t | \mathcal{R}_{t-1}] = r_t, \quad (4)$$

i.e., $(r_t)_{t=1}^{\infty}$ is the (unknown) conditional mean sequence of the outcomes. It is important to note that we place no distributional assumptions on $(r_t)_{t=1}^{\infty}$, such as stationarity, Markovian, and other conditional independence assumptions, so that the inference procedures we derive later are *distribution-free*. The simplest example of reality's filtration would be $\mathcal{R}_{t-1} = \sigma(r_1, \dots, r_t)$, i.e., the smallest σ -field generated by the reality sequence up to t , meaning reality makes its choice only based on its previous choices. More generally, we allow reality to choose r_t also using previous outcomes y_1, \dots, y_{t-1} , and we even allow r_t to be chosen adversarially, in the sense that r_t can be chosen after the forecasts p_t and q_t are made.

The Game Filtration $(\mathcal{G}_t)_{t=1}^{\infty}$. Finally, the game filtration $(\mathcal{G}_t)_{t=1}^{\infty}$ represents the all-encompassing information set with which the outcomes $(y_t)_{t=1}^{\infty}$ are realized in Game 1. It is with this filtration which we, as statisticians trying to compare the two forecasters involved in the game, conduct our analysis. The game filtration includes both the forecasters' and reality's filtrations, i.e., $\mathcal{G}_t \supset \mathcal{F}_t$ and $\mathcal{G}_t \supset \mathcal{R}_t$ for each $t \geq 1$, and thus $(p_t)_{t=1}^{\infty}$, $(q_t)_{t=1}^{\infty}$, and $(r_t)_{t=1}^{\infty}$ are predictable w.r.t. $(\mathcal{G}_t)_{t=1}^{\infty}$. We also have the equivalent of equation (4) for this larger filtration:

$$\mathbb{E}[y_t | \mathcal{G}_{t-1}] = r_t. \quad (5)$$

That is, for each $t \geq 1$, r_t is the mean of y_t conditional on the game filtration \mathcal{G}_{t-1} .

Comparing Sequential Forecasters via Average Forecast Score Differentials. Having defined the filtrations, we can now use scoring rules to assess compare the quality of the two forecasters over time. Following the formulation by Lai et al. (2011), we define the *average (forecast) score differential* Δ_t between the sequences of forecasts $(p_i)_{i=1}^{\infty}$ and $(q_i)_{i=1}^{\infty}$, up to time t , as follows:

$$\Delta_t := \frac{1}{t} \sum_{i=1}^t [S(p_i, r_i) - S(q_i, r_i)]. \quad (6)$$

The time-varying parameter Δ_t provides an intuitive way of quantifying the difference in the quality of forecasts made up to time t . It is important to note that Δ_t quantifies how much one forecaster is better than the other *on average* (of time), as opposed to one strictly

dominating the other (Giacomini and White, 2006; Henzi and Ziegel, 2021). We also note that, if S is bounded, e.g., when it is the Brier score, then $S(p, r) - S(q, r)$ is also bounded for any $p, q, r \in [0, 1]$.

Note that Δ_t is not observable to the forecasters or statistician, because reality's moves r_1, \dots, r_t are unknown and never observed. We thus define the *empirical average (forecast) score differential* $\hat{\Delta}_t$ using the actual outcomes y_1, \dots, y_t instead:

$$\hat{\Delta}_t := \frac{1}{t} \sum_{i=1}^t [S(p_i, y_i) - S(q_i, y_i)]. \quad (7)$$

Our goal as the statistician then becomes quantifying how far $\hat{\Delta}_t$ is from Δ_t , while accounting for uncertainty associated with sampling y_t at each time t . To achieve this goal, we define the *pointwise (forecast) score differential* $\delta_i := S(p_i, r_i) - S(q_i, r_i)$ as well as its empirical counterpart $\hat{\delta}_i := S(p_i, y_i) - S(q_i, y_i)$. In the following sections, we establish conditions with which the the difference sequence $(\hat{\delta}_i - \delta_i)_{i=1}^\infty$ forms a martingale difference sequence (MDS), such that their cumulative sums $t(\hat{\Delta}_t - \Delta_t)$ can be uniformly bounded via a nonnegative supermartingale. As a result, we will be able to estimate and cover Δ_t using confidence sequences that only depend on observable quantities.

3.3 Scoring Rules with Linear Equivalents

The key condition to deriving a valid CS for comparing forecasters is to consider scoring rules with linear equivalents. Following Lai et al. (2011), we say that a scoring rule S has a *linear equivalent* \tilde{S} if, for any p and r , $\tilde{S}(p, r)$ is a linear function of r and $S(p, r) - \tilde{S}(p, r)$ does not depend on p . For example, the Brier score $S(p, r) = -(p - r)^2$ has a linear equivalent $\tilde{S}(p, r) = 2pr - p^2$.⁷ Also, any scoring rule S that is already linear in r , such as the spherical score and the zero-one score, trivially has a linear equivalent ($\tilde{S} = S$). By definition, if a scoring rule has a linear equivalent, then we can compute the difference in scores between two forecasters only using the linear equivalents.

Scoring rules with linear equivalents satisfy the key condition for our forthcoming CSs.

Lemma 1 (Lai et al. (2011)). *If S has a linear equivalent, then for each $i \geq 1$,*

$$\mathbb{E} \left[\hat{\delta}_i \mid \mathcal{G}_{i-1} \right] = \delta_i. \quad (8)$$

The proof, provided in Appendix B.1, is a simple application of the definition of linear equivalents and the linearity of expectation. To be clear, the condition (8) essentially implies that the sequence $(\hat{\delta}_i - \delta_i)_{i=1}^\infty$ forms a martingale difference sequence w.r.t. $(\mathcal{G}_t)_{t=1}^\infty$. Lai et al. (2011) established this fact and used the martingale central limit theorem to obtain asymptotic CIs for Δ_n with fixed sample size n . Building upon this result, we now apply time-uniform bounds using nonnegative supermartingales to obtain anytime-valid and nonasymptotic CSs, which we describe in the next section.

⁷The logarithmic scoring rule $S(p, r) = r \log p + (1 - r) \log(1 - p)$ can also be viewed as a linear equivalent of the (negative) Kullback-Leibler divergence $S_{\text{KL}}(p, r) = -r \log \frac{r}{p} - (1 - r) \log \frac{1-r}{1-p}$. We focus on the Brier score in our subsequent analysis, however, because the logarithmic score is unbounded.

3.4 Time-Uniform Confidence Sequences for Δ_t

3.4.1 Time-uniform Boundaries and Exponential Supermartingales

Given a scoring rule with a linear equivalent, we now show that we can uniformly bound the difference between $\hat{\Delta}_t$ and Δ_t over time using uniform boundaries and nonnegative supermartingales. To do this, we first define the *cumulative sum* $S_t := \sum_{i=1}^t (\hat{\delta}_i - \delta_i)$ as well as its *intrinsic time* \hat{V}_t , which represents an estimate of the variance process for the cumulative sum S_t . Our goal is then to uniformly bound the sum S_t over the intrinsic time \hat{V}_t , which corresponds to bounding the difference between $\hat{\Delta}_t$ and Δ_t over time, as $\hat{\Delta}_t - \Delta_t = \frac{1}{t} \sum_{i=1}^t (\hat{\delta}_i - \delta_i) = S_t/t$. Note that $(S_t)_{t=1}^\infty$ and $(\hat{V}_t)_{t=1}^\infty$ are adapted to $(\mathcal{G}_t)_{t=1}^\infty$.

Given the sums $(S_t)_{t=1}^\infty$ and their intrinsic times $(\hat{V}_t)_{t=1}^\infty$, we define a *uniform boundary* $u = u_\alpha$ as any function of the intrinsic times that gives a time-uniform bound on the sums: for any $\alpha \in (0, 1)$,

$$\mathbb{P} \left(\forall t \geq 1 : S_t \leq u_\alpha(\hat{V}_t) \right) \geq 1 - \alpha, \quad (9)$$

i.e., with high probability, the sums S_t are upper-bounded by $u(\hat{V}_t)$ at all times t . By applying the same uniform boundary to $-S_t$, we can also obtain a time-uniform lower bound on S_t . We defer a more formal definition of uniform boundaries in Appendix A.

How do we show that there exists such a uniform boundary for our definitions of S_t and \hat{V}_t ? Howard et al. (2020, 2021) show that there exists a uniform boundary for (S_t, \hat{V}_t) if

$$L_t(\lambda) = \exp \left\{ \lambda S_t - \psi(\lambda) \hat{V}_t \right\} \quad (10)$$

is a supermartingale for each $\lambda \in [0, \lambda_{\max}]$, where $\psi : [0, \lambda_{\max}] \rightarrow \mathbb{R}$ is a cumulant generative function (CGF) of a random variable, such as the Gaussian CGF $\psi_N(\lambda) = \frac{\lambda^2}{2}$, the exponential CGF $\psi_{E,c}(\lambda) = c^{-2}(-\log(1-c\lambda) - c\lambda)$, and the gamma CGF $\psi_{G,c}(\lambda) = \frac{\lambda^2}{2(1-c\lambda)}$. The uniform boundary u for a CGF ψ in this construction is also called a *sub- ψ uniform boundary* (or sub-Gaussian, sub-exponential, and sub-gamma uniform boundaries if the CGF corresponds to a Gaussian, exponential, and gamma respectively).

Our goal is now to identify the conditions in which $L_t(\lambda)$ is indeed a supermartingale and use different CGFs to obtain different uniform boundaries and hence CSs. The resulting CSs all lead to an anytime-valid sequential inference procedure for Δ_t , with virtually no distributional assumptions on the outcomes or the forecasts.

3.4.2 Warmup: Hoeffding-Style Confidence Sequences for Δ_t

We first derive an illustrative example of a CS for Δ_t solely based on the sub-Gaussianity of the pointwise score differentials $(\hat{\delta}_i)_{i=1}^\infty$. While the resulting CS is not the tightest one in our case, its derivation is simple enough to showcase the general pipeline for deriving CSs.

Recall the problem setup in Section 3.2. For each $i \geq 1$, given that the probability forecasts $p_i, q_i \in [0, 1]$ as well as the binary outcome $y_i \in \{0, 1\}$ and its unknown mean $r_i \in [0, 1]$ are all bounded, we know that the pointwise score differentials $\hat{\delta}_i$ and δ_i are bounded (between -1 and 1 , specifically) for many of the scoring rules we've discussed (e.g., the Brier score, the spherical score, and the zero-one score). This implies that, assuming (8), we have that $\hat{\delta}_i$ is 1-sub-Gaussian⁸ conditioned on \mathcal{G}_{i-1} , meaning that $\mathbb{E}[e^{\lambda(\hat{\delta}_i - \delta_i)} \mid \mathcal{G}_{i-1}] \leq e^{\lambda^2/2}$ for all $\lambda \in \mathbb{R}$,

⁸See, e.g., Example 2.4 as well as Exercise 2.4 in Wainwright (2019).

or equivalently,

$$\mathbb{E} \left[\exp \left\{ \lambda \left(\hat{\delta}_i - \delta_i \right) - \psi_N(\lambda) \right\} \mid \mathcal{G}_{i-1} \right] \leq 1, \quad \forall \lambda \in \mathbb{R}, \quad (11)$$

where $\psi_N(\lambda) = \frac{\lambda^2}{2}$ is the Gaussian CGF.

Now, assuming $|\hat{\delta}_i| \leq 1$ for each i , and simply define the intrinsic time as $\hat{V}_t = \sum_{i=1}^t 1 = t$. It then follows that, for each $\lambda \in [0, \infty)$, the exponential process $L_t(\lambda) = \exp\{\lambda S_t - \psi_N(\lambda) \hat{V}_t\}$ is a supermartingale:

$$\mathbb{E} [L_t(\lambda) \mid \mathcal{G}_{t-1}] = L_{t-1}(\lambda) \cdot \mathbb{E} \left[\exp \left\{ \lambda \left(\hat{\delta}_t - \delta_t \right) - \psi_N(\lambda) \cdot 1 \right\} \mid \mathcal{G}_{t-1} \right] \leq L_{t-1}(\lambda). \quad (12)$$

Hence, there exists a sub-Gaussian uniform boundary for (S_t, \hat{V}_t) such that (9) holds. We summarize the result in the following theorem. We use the notation $(a \pm b)$ to denote the confidence interval $(a - b, a + b)$.

Theorem 1 (Hoeffding-Style Confidence Sequences for Δ_t). *Suppose that $\mathbb{E}[\hat{\delta}_i \mid \mathcal{G}_{i-1}] = \delta_i$ and $|\hat{\delta}_i| \leq 1$ for each $i \geq 1$. Then, for any $\alpha \in (0, 1)$,*

$$C_t^H := \left(\hat{\Delta}_t \pm \frac{u(t)}{t} \right) \quad \text{forms a } (1 - \alpha)\text{-CS for } \Delta_t, \quad (13)$$

where $u = u_{\alpha/2}$ is any sub-Gaussian uniform boundary with crossing probability $\alpha/2$.

The statement (13) is equivalent to saying that, with probability at least $1 - \alpha$, Δ_t is contained in C_t^H for all time t , or that $\mathbb{P}(\forall t \geq 1 : \Delta_t \in C_t^H) \geq 1 - \alpha$. This CS is called a Hoeffding-style CS, as it extends Hoeffding's inequality for the sums of independent sub-Gaussian random variables (Hoeffding, 1963) to the sequential case. Note that the conditions are satisfied when using scoring rules that have linear equivalents (Lemma 1) and are bounded on $[0, 1] \times [0, 1]$, including the Brier score, the spherical score, and the zero-one score. For the unbounded logarithmic score, one can use its truncated variant $S(p, r) = r \log(p \vee \epsilon) + (1 - r) \log(1 - (p \vee \epsilon))$ for some small $\epsilon > 0$, although the score is no longer proper. As for the choice of the sub-Gaussian uniform boundary u , we defer our discussion to Section 3.4.4.

3.4.3 Main Result: Empirical Bernstein Confidence Sequences for Δ_t

Now we are ready to present our main result, which is the derivation of a tight CS for Δ_t . The key difference from the Hoeffding-style CS is that we now use an empirical estimate of the variance process for the cumulative sums, leading to an empirical Bernstein (EB) CS.⁹

Recall the problem setup in Section 3.2 once again.

Theorem 2 (Empirical Bernstein Confidence Sequences for Δ_t). *Suppose that $\mathbb{E}[\hat{\delta}_i \mid \mathcal{G}_{i-1}] = \delta_i$ and $|\hat{\delta}_i| \leq \frac{c}{2} < \infty$ for each $i \geq 1$. Also, let $\hat{V}_t = \sum_{i=1}^t (\hat{\delta}_i - \gamma_i)^2$, where $(\gamma_i)_{i=1}^\infty$ is any $[-\frac{c}{2}, \frac{c}{2}]$ -valued predictable sequence w.r.t. $(\mathcal{G}_i)_{i=1}^\infty$. Then, for any $\alpha \in (0, 1)$,*

$$C_t^{\text{EB}} := \left(\hat{\Delta}_t \pm \frac{u(\hat{V}_t)}{t} \right) \quad \text{forms a } (1 - \alpha)\text{-CS for } \Delta_t, \quad (14)$$

where $u = u_{\alpha/2, c}$ is any sub-exponential uniform boundary with crossing probability $\alpha/2$ and scale c .

⁹The improvement from a Hoeffding-style CS to a empirical Bernstein CS mirrors the improvement from Hoeffding's inequality for independent sub-Gaussian random variables to empirical Bernstein's inequality for independent sub-exponential random variables in the fixed-sample case. Also note that sub-Gaussian random variables are sub-exponential. See, e.g., Section 2.1 of Wainwright (2019), for a review.

Type	CS C_t	Intrinsic Time \hat{V}_t	Uniform Boundary u
Hoeffding-Style (Theorem 1)	$\left(\hat{\Delta}_t \pm \frac{u(\hat{V}_t)}{t}\right)$	t	Polynomial Stitching Normal Mixture
Emp. Bernstein (Theorem 2)	$\left(\hat{\Delta}_t \pm \frac{u(\hat{V}_t)}{t}\right)$	$\sum_{i=1}^t (\hat{\delta}_i - \gamma_i)^2$, $(\gamma_i)_{i=1}^\infty$ predictable	Polynomial Stitching Gamma-Exponential Mixture

Table 3: Summary of confidence sequences and their uniform boundary choices.

As before, the statement (14) is equivalent to saying that, with probability at least $1 - \alpha$, Δ_t is contained in C_t^{EB} for all time t , or that $\mathbb{P}(\forall t \geq 1 : \Delta_t \in C_t^{\text{EB}}) \geq 1 - \alpha$. The proof is provided in Appendix B.2. Theorem 2 (and its proof) can be viewed as an extension of Theorem 4 in [Howard et al. \(2021\)](#) to our setup of sequential forecast comparison.

We highlight that Theorem 2 matches all the desiderata described in Section 3.1. Notably, it holds for virtually *any* sequence of probability forecasts and for *any* sequence of outcomes, without any stationarity or conditional independence assumptions on the outcomes (“distribution-free”), and it remains true even when the outcomes are chosen adversarially after the forecasts are already made. There are also no assumptions on the forecasts, as long as they are made without already knowing the outcome (which cannot happen in realistic forecasting tasks). Our confidence sequences therefore provide a virtually assumption-free sequential inference procedure for comparing probability forecasters over time.

As in Theorem 1, Lemma 1 gives the first condition for Theorem 2, meaning that we can use any bounded scoring rule with linear equivalents, including the Brier score, the spherical score, and the zero-one score (proper), as well as the truncated logarithmic score (improper). We will also show in Section 4.4 that a normalized version of the score ([Winkler, 1994](#)) can be used.

A reasonable choice for the predictable sequence $(\gamma_i)_{i=1}^\infty$ is the average of previous score differentials, i.e., $\gamma_i = \hat{\Delta}_{i-1}$, although a smarter choice may lead to tighter CS. We use $\gamma_i = \hat{\Delta}_{i-1}$ throughout our experiments in this paper. The choice of the uniform boundary u is discussed in the following subsection.

For the rest of this paper, our default choice of CS for Δ_t will be that of Theorem 2, using $\hat{V}_t = \sum_{i=1}^t (\hat{\delta}_i - \hat{\Delta}_{i-1})^2$, unless specified otherwise.

3.4.4 Choosing the Uniform Boundary u

The specific choice of the uniform boundary u controls the tightness of the CS across time, and the extensive list of choices for u is covered in detail in [Howard et al. \(2021\)](#). While the simplest uniform boundaries are given as a linear function of the intrinsic time, curved uniform boundaries can produce CSs that are tighter across time. Here, we focus on two curved boundaries, applicable to both Theorems 1 and 2: the *polynomial stitching boundary* and the *conjugate-mixture (CM) boundary*.

First, the polynomial stitched boundary provides a closed-form bound on the difference in estimated and actual forecast score differentials. It is constructed by finding a smooth analytical upper bound on a sequence of linear uniform bounds across different timesteps. The polynomial stitched boundary, which we denote as $u_\alpha^S(v)$, asymptotically grows with $O(\sqrt{v \log \log v})$ rate, matching the form of the law of the iterated logarithm (LIL). For example,

the 95% CS for Δ_t is given as follows (assuming $|\hat{\delta}_t - \delta_t| \leq 2$ for all $t \geq 1$):

$$\hat{\Delta}_t \pm 2 \cdot \frac{1.7 \sqrt{(\hat{V}_t \vee 1) (\log \log (2 (\hat{V}_t \vee 1)) + 3.8)} + 3.4 \log \log (2 (\hat{V}_t \vee 1)) + 13}{t} \quad (15)$$

where \hat{V}_t is the intrinsic time and $a \vee b = \max\{a, b\}$. Note that the width of the CS, given by $\frac{2}{t} u_{\alpha/2}^S(\hat{V}_t)$, shrinks toward zero at a $O(1/\sqrt{t})$ rate up to logarithmic factors, which is characteristic of CSs based on uniform boundaries.

The polynomial stitched boundary can be applied to both Theorems 1 and 2 by setting $\hat{V}_t = t$ and $\hat{V}_t = \sum_{i=1}^t (\hat{\delta}_i - \gamma_i)^2$ respectively: previous work has shown that the polynomial stitched boundary is a sub-gamma uniform boundary (Theorem 1, [Howard et al. \(2021\)](#)), and also that a sub-gamma uniform boundary is also a sub-Gaussian and a sub-exponential uniform boundary ([Proposition 1, Howard et al. \(2020\)](#)).

The second choice of u , which is our default choice in our subsequent experiments, is the CM boundary. The CM boundary represents a class of uniform boundaries arising from the following lemma:

Lemma 2 ([Lemma 2, Howard et al. \(2021\)](#)). *Given a CGF $\psi : [0, \lambda_{\max}] \rightarrow [0, \infty)$, a probability distribution F on $[0, \lambda_{\max}]$, and $\alpha \in (0, 1)$,*

$$u_{\alpha}^{\text{CM}}(v; \psi) := \sup \left\{ s \in \mathbb{R} : \underbrace{\int \exp \{ \lambda s - \psi(\lambda) v \} dF(\lambda)}_{=: m(s, v)} < \frac{1}{\alpha} \right\} \quad (16)$$

is a sub- ψ uniform boundary with crossing probability α , so long as the supermartingale $(L_t(\lambda))_{t=1}^{\infty}$ in (10) is product measurable with respect to $(\mathcal{G}_t)_{t=1}^{\infty}$ and the independent random variable λ .

The term $\exp\{\lambda s - \psi(\lambda) v\}$ inside the integral in (16) can be viewed as the supermartingale $L_t(\lambda)$ in (10), and the proof of Lemma 2 essentially involves showing that the integral $m(s, v)$ is also a supermartingale if $L_t(\lambda)$ is a supermartingale for each λ . Then, given a specific choice of ψ (e.g., Gaussian and exponential), we can choose F as the conjugate distribution (e.g., Gaussian and gamma) to evaluate the integral $m(s, v)$ in closed-form.

In the case where ψ is the Gaussian CGF, corresponding to the Hoeffding-style CS in Theorem 1, the sub-Gaussian CM boundary itself can also be computed in closed-form:

$$u_{\alpha}^{\text{CM}}(v; \psi_N) = \sqrt{(v + \rho) \log \left(\frac{v + \rho}{\alpha^2 \rho} \right)} \quad (17)$$

where $\rho > 0$ is a hyperparameter that controls the intrinsic time at which the bound can be its tightest. This boundary corresponds to the classical *normal mixture* by [Robbins \(1970\)](#).

In the case of the exponential CGF, corresponding to the empirical Bernstein CS in Theorem 2, the sub-exponential CM boundary $u_{\alpha}^{\text{CM}}(v; \psi_E)$ does not have a closed form (the integral $m(s, v)$ does have a closed form, but the boundary $u_{\alpha}^{\text{CM}}(v; \psi_E)$ does not), although in practice it can still be computed efficiently using a numerical root finder. As the sub-exponential CM boundary uses the gamma-exponential conjugacy, we also refer to it as the *gamma-exponential mixture* uniform boundary. Also, while the CM boundary has an asymptotic rate of $O(\sqrt{v \log v})$ as illustrated in (17), it is usually tighter than the polynomial stitched

boundary in practice. In fact, the CM boundary is shown to be unimprovable in the case of sub-Gaussian random variables unless more assumptions are made (Proposition 4, [Howard et al. \(2021\)](#)).

[Table 3](#) summarizes the choice of uniform boundaries and the CSs we derived for estimating Δ_t . In our experiments, we mostly use the appropriate CM boundary, although we also perform an empirical comparison between the different choices as well as their hyperparameters in [Appendix D](#). Finally, we note that we use the publicly available implementation of the polynomial stitching and CM uniform boundaries by [Howard et al. \(2021\)](#).¹⁰

3.5 e-Processes and Anytime-Valid p-Processes

While our derivation so far has focused on confidence sequences, we can also derive e-processes and anytime-valid p-processes ([Shafer and Vovk, 2019](#); [Vovk and Wang, 2021](#); [Grünwald et al., 2019](#); [Ramdas et al., 2020](#)), using the exponential supermartingale (10) that we used to construct the CS in the previous section. This correspondence is general to any exponential process upper-bounded by a NSM, as noted in, e.g., [Ramdas et al. \(2020\)](#); [Howard et al. \(2021\)](#). For the sake of exposition, we illustrate this correspondence in the case of the CS derived in [Theorem 2](#).

Weak and Strong Null Hypotheses. Before deriving e- and p-processes, we must first make clear the null hypotheses that correspond to the CS derived in [Theorem 2](#). We define the *weak one-sided null* $H_0^w(p, q)$ as

$$H_0^w(p, q) : \Delta_t = \frac{1}{t} \sum_{i=1}^t \delta_i = \frac{1}{t} \sum_{i=1}^t \mathbb{E} \left[\hat{\delta}_i \mid \mathcal{G}_{i-1} \right] \leq 0. \quad (18)$$

$H_0^w(p, q)$ corresponds to saying that the first forecaster (p) is no better than the second forecaster (q) *on average* up to a non-prespecified time t . $H_0^w(q, p)$ is analogously defined as $H_0^w(q, p) : -\Delta_t = -\frac{1}{t} \sum_{i=1}^t \delta_i \leq 0$.

Our confidence sequences derived in [Theorem 1](#) and [Theorem 2](#) would correspond to sequential tests for both of the weak one-sided nulls $H_0^w(p, q)$ and $H_0^w(q, p)$, as they have a time-uniform coverage guarantee for the quantity Δ_t . Specifically, because the lower and upper confidence bounds of our CSs are constructed separately, the $(1 - \alpha)$ -level CS for Δ_t denoted as $C_t = (L_t, U_t)$ satisfies $\Delta_t \leq U_t$ with probability at least $1 - \frac{\alpha}{2}$ and that $\Delta_t \geq L_t$ with probability at least $1 - \frac{\alpha}{2}$. Thus, if for any time t we find that $L_t > 0$ or $U_t < 0$, then we can reject either $H_0^w(p, q)$ or $H_0^w(q, p)$ with high probability. In other words, the CSs readily provide a valid stopping rule for rejecting H_0^w :

$$\text{Reject } H_0^w(p, q) \text{ if } L_t > 0; \text{ reject } H_0^w(q, p) \text{ if } U_t < 0. \quad (19)$$

The stopping rule (19) is equivalent to *deciding that p is better (worse) than q if C_t is entirely above (below) zero*. This is useful when making inferential conclusions, as we illustrate in [Section 5](#).

We also define the *strong one-sided null* $H_0^s = H_0^s(p, q)$ as

$$H_0^s(p, q) : \delta_i = \mathbb{E} \left[\hat{\delta}_i \mid \mathcal{G}_{i-1} \right] \leq 0 \quad \forall i = 1, \dots, t. \quad (20)$$

¹⁰<https://github.com/gostevehoward/confseq>

$H_0^s(q, p)$ is defined analogously as $H_0^s(q, p) : -\delta_i \leq 0 \ \forall i = 1, \dots, t$. In contrast to H_0^w , H_0^s corresponds to saying that the first forecaster (p) is no better than the second forecaster (q) *at every time step* $i = 1, \dots, t$. Thus, the strong null H_0^s implies the weak null H_0^w , but not vice versa. The critical distinction here is that rejecting $H_0^s(p, q)$ only tells us that the first forecaster outperformed the second one at some time step i , but it does not tell us if either was better over the rounds that we've observed. Notably, the recent work by [Henzi and Ziegel \(2021\)](#) provides sequential inference procedures for the strong one-sided null, contrasting with our approach that involves the weak version.

Note that, in a sequential setting where inference can be made for every time step t , the two-sided versions of H_0^w and H_0^s would coincide as the strong two-sided null, as both versions would imply that $\delta_i = 0 \ \forall i = 1, \dots, t$ when applied over time. Importantly, the sequential test implied by our CS from Theorem 2 is *not* a test of the strong two-sided null but of two weak one-sided nulls, combined into one CS via a union bound.

e-Processes via Exponential Supermartingales. Having defined the null hypotheses, we can now show that the exponential supermartingale underlying the construction of our CSs in Theorem 2 can be used to construct a sequence of random variables that measure the accumulated evidence against the weak one-sided null. Formally, an *e-process* ([Ramdas et al., 2021](#)) for the null H_0 is defined as a nonnegative sequence of random variables $(E_t)_{t=1}^\infty$, adapted to $(\mathcal{G}_t)_{t=1}^\infty$, such that under H_0 , the following holds:

$$\text{for any arbitrary stopping time } \tau, \quad \mathbb{E}_{H_0}[E_\tau] \leq 1, \quad (21)$$

where we take $E_\infty = \limsup_{t \rightarrow \infty} E_t$ for infinite stopping times. The term ‘process’ is used to emphasize the fact that the condition $\mathbb{E}_{H_0}[E_\tau] \leq 1$ is true under H_0 at arbitrary *stopping times*. Importantly, the time-uniform coverage guarantee for CSs is *equivalent* to coverage guarantees at arbitrary stopping times ([Lemma 3, Howard et al. \(2021\)](#); [Proposition 1, Zhao et al. \(2016\)](#)), such that our CSs derived for arbitrary (not necessarily stopping) times also have coverage guarantees at stopping times. For each t , E_t is also called an e-variable, and its realization is called an e-value ([Vovk and Wang, 2021](#); [Grünwald et al., 2019](#)). The notion of measuring evidence against the null directly corresponds to increasing one’s wealth by betting against the null in game-theoretic statistics ([Shafer, 2021](#)).

We can now define and show an e-process that corresponds to Theorem 2. Recall once again the problem setup in Section 3.2.

Theorem 3 (Sub-exponential e-Processes for H_0^w). *Assume the same conditions as Theorem 2. Then, for each $\lambda \in [0, \lambda_{\max}]$,*

$$E_t(\lambda) := \exp \left\{ \lambda \sum_{i=1}^t \hat{\delta}_i - \psi_{E,c}(\lambda) \hat{V}_t \right\} \quad \text{is an e-process for } H_0^w(p, q), \quad (22)$$

where $\psi_{E,c}$ is the sub-exponential CGF with scale c .

The proof, provided in Appendix B.3, shows that under H_0^w , $E_t(\lambda)$ is upper-bounded by the supermartingale analogous to $L_t(\lambda)$ in (10) now computed using $\lambda_1, \dots, \lambda_t$. For any choice of λ and any stopping time τ , $E_\tau(\lambda)$ provides a measure of accumulated evidence against the weak one-sided null $H_0^w(p, q)$, leading to an alternative sequential inference procedure for sequentially comparing forecasters in terms of their average performance over time. Also, note that for each t and $i = 1, \dots, t$, E_t can be calculated only using the forecasts p_i, q_i and the

observed outcomes y_i , assuming γ_i is also computed using them (e.g., $\gamma_i = \hat{\Delta}_{i-1}$). Theorem 3 further allows us to directly compare our approach with [Henzi and Ziegel \(2021\)](#)'s e-processes for the strong one-sided null $H_0^s(p, q)$; we later provide an empirical comparison of the two procedures in Section 5.3.

Choosing λ for e-Processes. Choosing λ for $E_t(\lambda)$ in Theorem 3 is an easier task than choosing a uniform boundary u for C_t in Theorems 1 or 2, as it can be done within the first step of choosing a uniform boundary. This is because the first step of choosing a uniform boundary for a CS, as described in Section 3.4.4, corresponds to constructing the underlying supermartingale $L_t(\lambda)$ with the appropriate λ , which we can directly use for our e-processes.

For example, when using the CM boundary, which is our default choice, the integral $m(s, v)$ from (16) evaluated at $(\sum_{i=1}^t \hat{\delta}_i, \hat{V}_t)$ directly gives us the e-value at time t , where F is the conjugate distribution (Gaussian for Theorem 1; gamma for Theorem 2). Note that the integral $m(s, v)$ can be computed in closed-form for any CM boundaries, including the normal mixture and the gamma-exponential mixture¹¹, even when the uniform boundary (16) cannot. The polynomial stitched bound also yields a form that corresponds to a discrete mixture (Theorem 2 in [Howard et al. \(2021\)](#)), such that a discrete sum (instead of an integral for CM) can be computed to give the e-value directly.

Anytime-Valid p-Processes. Finally, we also note that any e-process for H_0 can also be converted into an *anytime-valid p-process* for H_0 , which is defined as the sequence $(p_t)_{t=1}^\infty$ that satisfies, for any $\alpha \in (0, 1)$:

$$\text{for any arbitrary stopping time } \tau, \quad \mathbb{P}_{H_0}(p_\tau \leq \alpha) \leq \alpha. \quad (23)$$

Given an e-process $(E_t)_{t=1}^\infty$, we can convert it into an anytime-valid p-process via

$$p_t := \inf_{i \leq t} 1/E_i. \quad (24)$$

following derivations from, e.g., [Ramdas et al. \(2020, 2021\)](#). p_t can alternatively be defined from a CS as the smallest α for which the $(1 - \alpha)$ -level CS does not include zero ([Howard et al., 2021](#)), so all three notions (CS, e-values, and anytime-valid p-values) are closely related.

4 Extensions

In this section, we discuss a set of extensions that allow us to perform anytime-valid sequential forecast comparison beyond the case of probability forecasts on binary outcomes. While our derivation and experiments so far focused on the case of binary outcomes using the Brier score, Theorem 1 and Theorem 2 can be extended to other cases, some more readily than others. At a high level, the key is to consider other sequential forecasting scenarios where the condition (8) continues to hold.

4.1 Comparing Probabilistic Forecasts on Categorical Outcomes

In Section 3, our derivation of a CS for the average forecast score differential Δ_t focused on the case of binary outcomes. We now show that essentially the same derivation can be done for comparing probabilistic forecasts made on categorical outcomes with K classes. As a result, we

¹¹We derive the closed-form expression for the gamma-exponential mixture in Appendix C.

arrive at a time-uniform, non-asymptotic, and distribution-free sequential inference procedure for comparing two probabilistic forecasts on categorical outcomes without much additional work.

For each $t = 1, 2, \dots$, let $\mathbf{y}_t = (y_t^{(1)}, \dots, y_t^{(K)}) \in \{0, 1\}^K$ be the categorical outcome at time t represented as a one-hot vector (i.e., $\sum_{k=1}^K y_k = 1$). Let $\mathbf{p}_t = (p_t^{(1)}, \dots, p_t^{(K)}) \in \Delta^{K-1}$ and $\mathbf{q}_t = (q_t^{(1)}, \dots, q_t^{(K)}) \in \Delta^{K-1}$ be probabilistic forecasts made by two forecasters on \mathbf{y}_t , where Δ^{K-1} is the K -dimensional probability simplex (i.e., $p_t^{(k)} \in [0, 1]$ and $\sum_{k=1}^K p_t^{(k)} = 1$). Using these notations, we can set up an analogous game setup to Game 1:

Game 2 (Comparing Sequential Probabilistic Forecasts on Categorical Outcomes). *For rounds $t = 1, 2, \dots$:*

1. *Forecasters 1 and 2 make their probabilistic forecasts, $\mathbf{p}_t \in \Delta^{K-1}$ and $\mathbf{q}_t \in \Delta^{K-1}$, respectively.* The order in which the forecasters make their forecasts is not specified.
2. *Reality chooses $\mathbf{r}_t \in \Delta^{K-1}$.* Note that \mathbf{r}_t is not revealed to the forecasters.
3. $\mathbf{y}_t \sim \text{Categorical}(\mathbf{r}_t)$ is sampled and revealed to the forecasters.

This game is equivalent to Game 1 when $K = 2$, as we can use the one-hot representation of the binary outcomes and set $\mathbf{p}_t := (1 - p_t, p_t)$. The reality still plays the role of specifying the unknown mean of the outcomes by now specifying a K -categorical distribution. Generalizing the corresponding definitions of filtrations from Section 3.2 to these forecasts, we have the following analog of (5):

$$\mathbb{E}[\mathbf{y}_t | \mathcal{G}_{t-1}] = \mathbf{r}_t \quad \forall t. \quad (25)$$

The classical examples of proper scoring rules for binary outcomes, as well as their key properties, also generalize seamlessly to the categorical case.

- The Brier score or the quadratic score (Brier, 1950):

$$S(\mathbf{p}, \mathbf{r}) = -\|\mathbf{p} - \mathbf{r}\|_2^2.$$

- The spherical score (Good, 1971):

$$S(\mathbf{p}, \mathbf{r}) = \frac{\mathbf{p}^T \mathbf{r}}{\|\mathbf{p}\|_2}.$$

- The logarithmic score (Good, 1952):

$$S(\mathbf{p}, \mathbf{r}) = \log(\mathbf{p})^T \mathbf{r}.$$

- The zero-one score or the success rate:

$$S(\mathbf{p}, \mathbf{r}) = \mathbf{1}(\mathbf{p} \geq 0.5)^T \mathbf{r}.$$

where we define vector-valued evaluations of basic arithmetic functions by their elementwise application, i.e., $\log(\mathbf{p}) := (\log p^{(k)})_{k=1}^K$ and $\mathbf{1}(\mathbf{p} \geq 0.5) := (\mathbf{1}(p^{(k)} \geq 0.5))_{k=1}^K$. The Brier score has a linear equivalent in the form $\tilde{S}(\mathbf{p}, \mathbf{r}) = -\mathbf{p}^T \mathbf{p} + 2\mathbf{p}^T \mathbf{r}$, and the spherical, logarithmic, and zero-one scores are already linear in \mathbf{r} .

Using these scoring rules, we can analogously define the average forecast score differential Δ_t between $(\mathbf{p}_i)_{i=1}^\infty$ and $(\mathbf{q}_i)_{i=1}^\infty$ up to time t as

$$\Delta_t := \frac{1}{t} \sum_{i=1}^t [S(\mathbf{p}_i, \mathbf{r}_i) - S(\mathbf{q}_i, \mathbf{r}_i)]. \quad (26)$$

as well as its empirical estimate

$$\hat{\Delta}_t := \frac{1}{t} \sum_{i=1}^t [S(\mathbf{p}_i, \mathbf{y}_i) - S(\mathbf{q}_i, \mathbf{y}_i)]. \quad (27)$$

The pointwise differentials are also defined analogously, i.e., $\delta_i = S(\mathbf{p}_i, \mathbf{r}_i) - S(\mathbf{q}_i, \mathbf{r}_i)$ and $\hat{\delta}_i = S(\mathbf{p}_i, \mathbf{y}_i) - S(\mathbf{q}_i, \mathbf{y}_i)$ for each $i \geq 1$.

Then, given the same definitions of the score differentials as well as the categorical analogs of scoring rules with linear equivalents, it is clear that Lemma 1 as well as Theorems 1 and 2 still hold, meaning that the same time-uniform sequential inference procedures can be used for probabilistic forecasts on categorical outcomes.

4.2 Comparing k -Step-Ahead Forecasts

In many forecasting scenarios, it is common for forecasters to make k -step-ahead forecasts for an eventual binary or categorical outcome. For example, meteorologists would make 7-day forecasts each day, such that there are a total of seven forecasts made for each outcome (one made seven days ago, six days ago, and so on). To compare the overall performance of these forecasters over time, we consider a weighted average of their forecast scores. Assuming that we use scoring rules with linear equivalents, our derivation from Section 3 can readily be extended to the overall comparison of k -step-ahead forecasters. For notational simplicity, we focus on the case where the outcomes are binary, although an analogous extension to categorical outcomes will continue to hold as in Section 4.1.

For each $k = 1, \dots, K$, let $p_t^{(k)}$ and $q_t^{(k)}$ denote the k -step ahead probability forecasts by two forecasters on the eventual outcome y_t . Note that the forecasts $p_t^{(k)}$ and $q_t^{(k)}$ are made at the beginning of round $t - k + 1$. Then, Game 1 can be extended to k -step-ahead forecasts as follows:

Game 3 (Comparing Sequential k -Step-Ahead Forecasts on Binary Outcomes). *Fix $K \geq 1$. For rounds $t = 1, 2, \dots$:*

1. *Forecasters 1 and 2 make their k -step ahead probability forecasts, $p_t^{(1)}, p_{t+1}^{(2)}, \dots, p_{t+K-1}^{(K)} \in [0, 1]$ and $q_t^{(1)}, q_{t+1}^{(2)}, \dots, q_{t+K-1}^{(K)} \in [0, 1]$, respectively. The order in which the forecasters make their forecasts is not specified.*
2. *Reality chooses $r_t \in [0, 1]$. r_t is not revealed to the forecasters.*
3. *$y_t \sim \text{Bernoulli}(r_t)$ is sampled and revealed to the forecasters.*

Given a scoring rule S with a linear equivalent \tilde{S} , along with pre-determined weights $\mathbf{w} = (w_1, \dots, w_K) \in [0, 1]^K$ such that $\sum_{k=1}^K w_k = 1$, we can define the weighted average of the previous k -step forecast scores as the measure of overall performance as follows. Let $\mathbf{p}_t = (p_t^{(1)}, p_t^{(2)}, \dots, p_t^{(K)})$ be the vector containing the K most recent probability forecasts

made by a forecaster on the outcome y_t with mean r_t , sorted from the most recent to the least. Then, define

$$S_{\mathbf{w}}(\mathbf{p}_t, r_t) := \sum_{k=1}^K w_k S(p_t^{(k)}, r_t). \quad (28)$$

The scoring rule $S_{\mathbf{w}}$ now measures the overall quality of k -step ahead forecasts for $k = 1, \dots, K$, averaged using weights \mathbf{w} .¹² Given two sequences of k -step-ahead forecasts, $(\mathbf{p}_t)_{t=1}^{\infty}$ and $(\mathbf{q}_t)_{t=1}^{\infty}$, we can compare them by analogously constructing a CS for their average forecast score differentials $(\Delta_t)_{t=1}^{\infty}$, now using $S_{\mathbf{w}}$:

$$\Delta_t = \frac{1}{t} \sum_{i=1}^t [S_{\mathbf{w}}(\mathbf{p}_i, r_i) - S_{\mathbf{w}}(\mathbf{q}_i, r_i)]. \quad (29)$$

The empirical estimate is analogously defined as:

$$\hat{\Delta}_t = \frac{1}{t} \sum_{i=1}^t [S_{\mathbf{w}}(\mathbf{p}_i, y_i) - S_{\mathbf{w}}(\mathbf{q}_i, y_i)]. \quad (30)$$

With this definition of k -step-ahead forecasts and the scoring rule $S_{\mathbf{w}}$, we can derive an analog of Lemma 1, which then allows us to use the CS in Theorem 2.

Lemma 3. *Assume that S has a linear equivalent, and define $\delta_i = S_{\mathbf{w}}(\mathbf{p}_i, r_i) - S_{\mathbf{w}}(\mathbf{q}_i, r_i)$ and $\hat{\delta}_i = S_{\mathbf{w}}(\mathbf{p}_i, y_i) - S_{\mathbf{w}}(\mathbf{q}_i, y_i)$ for each $i \geq 1$. Then, for each $i \geq 1$,*

$$\mathbb{E} [\hat{\delta}_i \mid \mathcal{G}_{i-1}] = \delta_i. \quad (31)$$

The proof is provided in Appendix B.4. Lemma 3 shows that the condition for Theorems 1 and 2 also holds when comparing k -step-ahead forecasts according to the scoring rule (28), and thus we have a time-uniform CS for their average score differentials as well. We note that, at a stopping time τ , the resulting procedure will not take into account predictions of the future, say at time $\tau + k$ for some k , for which the actual outcome $y_{\tau+k}$ is not realized. This does not invalidate our procedure, as it would usually suffice to make comparisons based on realized outcomes only.

4.3 Comparing Mean Forecasts on (Bounded) Continuous Outcomes

Our derivation with binary outcomes and probability forecasts can also be extended to the case of forecasting the time-varying means of bounded continuous outcomes. In this case, reality is now assumed to choose an unknown distribution for the continuous outcome at each round t , such that the distribution has a time-varying mean parameter that the forecasters try to predict.¹³ This generalizes the case of binary outcomes, in the sense that the unknown parameter r_t is in fact the mean of the outcome y_t given \mathcal{G}_{t-1} , as in (5). We now state the corresponding game to compare the case of bounded continuous outcomes with that of binary outcomes.

¹²One can also verify that if S is proper, then $S_{\mathbf{w}}$ is also proper for $\mathbf{w} \in (0, 1)^K$, where we extend the definition of propriety to allow for vector-valued forecasts $\mathbf{p} \in [0, 1]^K$ in the first argument.

¹³Because the forecasters are assumed to predict the mean only, their forecasts are now viewed as deterministic, as opposed to probabilistic. In the case of binary outcomes, the two cases overlap, as the mean fully specifies the underlying distribution.

Game 4 (Comparing Sequential Forecasts on Means of Bounded Continuous Outcomes). *Let $a, b \in \mathbb{R}$ such that $a < b$. For rounds $t = 1, 2, \dots$:*

1. *Forecasters 1 and 2 make their k -step ahead probability forecasts, $p_t \in [a, b]$ and $q_t \in [a, b]$, respectively.* The order in which the forecasters make their forecasts is not specified.
2. *Reality chooses a distribution \mathcal{P}_t with mean $r_t \in [a, b]$. \mathcal{P}_t (or r_t) is not revealed to the forecasters.*
3. *$y_t \sim \mathcal{P}_t$ is sampled and revealed to the forecasters.*

As with Game 1, Game 4 is inherently sequential, and there are no assumptions of parametric models or stationarity made on the underlying distribution for outcomes. The key difference between the two games, however, is that the forecasters in Game 4 are assumed to predict only the mean of the underlying distribution, \mathcal{P}_t , which may no longer be fully specified by its mean. This is to ensure that the martingale property of the sums of estimated and actual score differentials continues to hold; extending this to fully probabilistic forecasts for continuous outcomes remains future work. We are also implicitly adding the assumption that the underlying distribution of outcomes has a mean, an assumption that we did not need for the binary case.

Unlike in the binary or the categorical case, the boundedness assumption on forecasts and outcomes is required for the sub-exponential uniform boundaries we use in Theorem 2. An alternative is to only assume sub-Gaussianity of the score differentials $\hat{\delta}_i = S(p_i, y_i) - S(q_i, y_i)$ and use Theorem 1 instead.

Assuming boundedness or sub-Gaussianity, we can readily extend the definitions of score differentials (6) and (7) to the case of mean forecasts on continuous outcomes, and combine Lemma 1 with either Theorem 2 (boundedness) or 1 (sub-Gaussianity) to obtain a time-uniform CS for Δ_t .

4.4 Winkler's Normalized Score Differentials

Focusing again on the case of binary outcomes, we now show that Theorems 1 and 2 can also be used to construct time-uniform CSs for a normalized version of average score differentials, also known as the Winkler score. Winkler (1994) provided a standardized scoring rule that measures the relative improvement of a given forecaster over an “unskilled” baseline forecaster, such as the historical average (referred to as *climatology* in weather forecasting) $c_t = c = \frac{1}{H} \sum_{h=-(H-1)}^0 y_h \forall t \geq 1$. This normalized version of the score can be viewed as a better reflection of the relative “skill” of a given forecaster (Winkler, 1994; Lai et al., 2011).

In our derivation, we slightly generalize the notion to allow any forecaster $(q_t)_{t=1}^\infty$ predictable w.r.t. $(\mathcal{G}_t)_{t=1}^\infty$ (and bounded away from 0 and 1) to be a baseline forecaster. For any $p, r \in [0, 1]$ and $q \in (0, 1)$, the *Winkler score* $w(p, q, r)$ can be defined as follows:

$$w(p, q, r) := \frac{S(p, r) - S(q, r)}{T(p, q)} \tag{32}$$

where $0/0 := 0$, and

$$\begin{aligned} T(p, q) &= S(p, \mathbf{1}(p \geq q)) - S(q, \mathbf{1}(p \geq q)) \\ &= [S(p, 1) - S(q, 1)] \mathbf{1}(p \geq q) + [S(p, 0) - S(q, 0)] \mathbf{1}(p < q) \end{aligned} \tag{33}$$

is a normalizer for the pointwise score differential.¹⁴ Here, we fix S to be the Brier score. Note that $T(p, q) \geq 0$ and $T(p, q) = 0$ iff $p = q$ (in which case $w(p, q, r) = 0$), due to the propriety of S .

Winkler (1994) notes that, given a baseline forecaster $q = c$, w itself is a strictly proper scoring rule for p if S is strictly proper, which is the case when S is the Brier score. The score is standardized in the sense that, if the binary outcome is in fact generated according to $y \sim \text{Bernoulli}(p)$, then the expected score w.r.t. the outcome i.e., $\mathbb{E}_{y \sim \text{Bernoulli}(p)}[w(p, q, y)]$, is minimized at zero for $p = q$ and maximized at 1 for $p = 0$ and $p = 1$.

We can now derive conditions for which we can also use Theorems 1 and 2 for the average of Winkler scores over time. For each time t , define $w_t = w(p_t, q_t, r_t)$ and $\hat{w}_t = w(p_t, q_t, y_t)$.

Lemma 4. *Suppose that, for each $t \geq 1$, $q_t \in (q_0, 1 - q_0)$ a.s. for some fixed $q_0 \in (0, 1)$. If S has a linear equivalent, then $\mathbb{E}[\hat{w}_t | \mathcal{G}_{t-1}] = w_t$ for each $i \geq 1$.*

The proof, provided in Appendix B.5, makes use of the fact that $(T(p_t, q_t))_{t=1}^\infty$ is predictable w.r.t. $(\mathcal{G}_t)_{t=1}^\infty$. The scalar q_0 determines the lower bound on the Winkler score. Given that S is the Brier score, the corresponding Winkler score has an upper bound of 1 and a lower bound of $1 - \frac{2}{q_0 \wedge (1 - q_0)}$ (happens when either $p = 0$ and $r = 1$ or $p = 1$ and $r = 0$).

We can now define the *average Winkler score* up to time t ,

$$W_t := \frac{1}{t} \sum_{i=1}^t w(p_i, q_i, r_i), \quad (34)$$

as well as its empirical estimate

$$\hat{W}_t := \frac{1}{t} \sum_{i=1}^t w(p_i, q_i, y_i), \quad (35)$$

for each $t \geq 1$. Then, by setting $\hat{\delta}_i \leftarrow \hat{w}_i$ and $\delta_i \leftarrow w_i$ in Theorem 1 or 2, we can also obtain a time-uniform CS for W_t . The average Winkler score W_t has an intuitive interpretation as a normalized version of the average score differential Δ_t in (6) or as the average “skill gap” between the two forecasters.

5 Experiments

In this section, we run both simulated and real-data experiments for sequential forecast comparison using our CSs as well as e-processes. All code and data sources for the experiments are made publicly available online at <https://github.com/yjchoe/ComparingForecasters>.

5.1 Simulated Experiments

As our first experiment, we empirically compare our CSs with the fixed-time CIs due to Lai et al. (2011) (Theorem 2). Importantly, the fixed-time CI is only valid at a time t fixed *a priori* and does not have a finite-sample coverage guarantee that the CS has. We also include an asymptotic CS, recently derived by Waudby-Smith et al. (2021) (Theorem 7), as another

¹⁴We note that this normalizer also appears in its absolute value as the e-value increment in (Henzi and Ziegel, 2021), i.e., $E(\lambda) = 1 + \lambda \frac{S(p, r) - S(q, r)}{|T(p, q)|}$. This means that we can interpret the amount of wealth gained by betting against the null in (Henzi and Ziegel, 2021) reflects the relative skill score, as Winkler’s score does.

baseline. This CS can be viewed as the asymptotic analog of our nonasymptotic version in Theorem 2 and only has asymptotic guarantees. In practice, the asymptotic CS is expected to be the “limit” of the nonasymptotic CS, in the sense that the width of the nonasymptotic CS approaches the width of the asymptotic CS as t increases.

As for our simulated data, we generate a sequence of non-IID binary outcomes and compare different forecasters using our CS. We generate the simulated data with $T = 10^4$ rounds, following a version of Game 1 with different pairs of forecasters and a non-IID reality sequence. At the end of each round $t = 1, \dots, T$, we compute the $(1 - \alpha)$ -level Hoeffding and EB CS for Δ_t , using Theorems 1 and 2 respectively. We use the Brier score $S(p, q) = -(p - q)^2$ as our default scoring rule, but we also explore other scoring rules later in the section.

The reality sequence $(r_t)_{t=1}^T$ is specifically chosen to be non-IID and contain sharp changepoints, as drawn with gray dots in Figure 2. It is specifically chosen as follows:

$$r_t = [0.8 \cdot \theta_t + 0.2 \cdot (1 - \theta_t)] + \epsilon_t,$$

where

$$\theta_t = \begin{cases} 0.5 & \text{for } t \in [1, 10^2] \\ 0 & \text{for } t \in (10^2, 0.5 \cdot 10^3] \\ 1 & \text{for } t \in (0.5 \cdot 10^3, 0.5 \cdot 10^4] \\ 0 & \text{for } t \in (0.5 \cdot 10^4, 10^4], \end{cases}$$

and $\epsilon_t \sim \mathcal{N}(0, 0.1^2)$ is an independent Gaussian noise for each t .

We also compare several forecasters, which are drawn with lines in Figure 2. These include constant baselines — $p_t = 0.5$ (`always_0.5`), $p_t = 0$ (`always_0`), and $p_t = 1$ (`always_1`) —, as well as the Laplace forecasting algorithm (`laplace`) $p_t = \frac{k+0.5}{t+1}$, where $k = \#\{i \in [t] : y_i = 1\}$. We also add predictions using the K29 defensive forecasting algorithm (Vovk et al., 2005), which is a game-theoretic forecasting method that leads to calibrated forecasts, using the polynomial kernel with degree $d = 3$ (`k29_poly3`), $K(p, q) = (1 + pq)^d$, and the Gaussian RBF kernel with noise $\sigma = 0.01$ (`k29_rbf0.01`), $K(p, q) = \exp\left(-\frac{(p-q)^2}{2\sigma^2}\right)$. Note that all of the forecasters only make use of the previous outcomes y_1, \dots, y_{t-1} , except for the constant baselines which do not use the outcomes.

Among the constant baselines, none of them are expected to dominate each other at the end, although the true Δ_t between them may change signs over time. For example, for $t \in (10^2, 0.5 \cdot 10^3)$, in which reality consistently favors the outcome 0, the `always_0` forecaster is expected to dominate over the `always_1` forecaster, although the sign will then reverse over the next span where reality consistently favors the outcome 1. Among the algorithmic forecasters, it is expected that the K29 variants will consistently perform better than the Laplace algorithm, especially when using ones with sharper kernels, because they should be better at modeling the sharp changepoints.

In Figure 1 and Figure 3, we plot the 95% Hoeffding and EB CSs, fixed-time CI, and asymptotic CS for Δ_t (left), along with their widths (right). We draw the plots for three illustrative cases: when one forecaster is strictly better than the other always (Figure 1), when the two forecasters are alternatingly good but no better than the other overall (Figure 3, top), and when one forecaster is typically but not always better than the other (Figure 3, bottom).

In all three cases, our CSs successfully cover Δ_t at any given time point, and their widths sharply decreases as more outcomes are observed. As expected, the width of the EB CS decays more quickly than the width of the Hoeffding CS. This trend, as well as the ratio between the width of the EB CS and its fixed-time counterpart, roughly matches the patterns observed

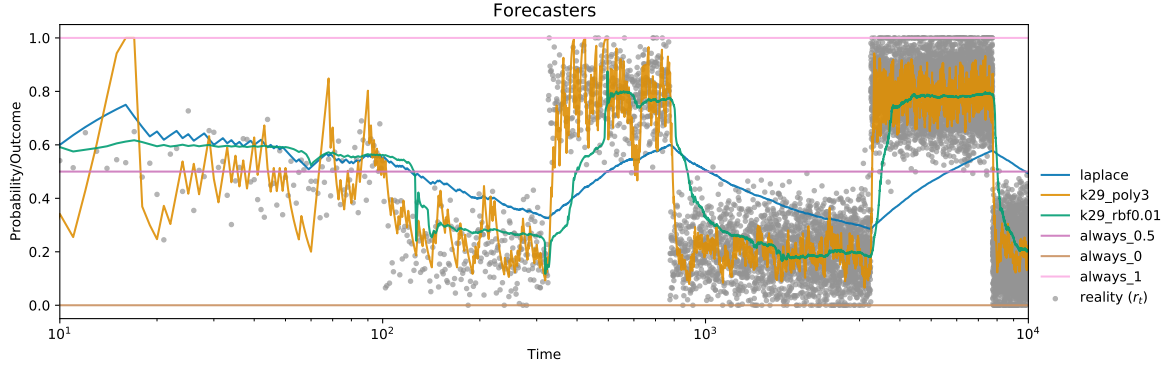


Figure 2: Various forecasters on a simulated non-IID data ($T = 10^4$) with sharp changepoints spaced out in log-scale. Note that, instead of plotting the binary outcomes $y_t \in \{0, 1\}$, we plot the reality sequence $(r_t)_{t=1}^T$ that generates the outcome sequence. See text for details about the forecasters.

in (Howard et al., 2021; Waudby-Smith et al., 2021). As noted before, the fixed-time CIs are only valid at a fixed time t and not uniformly over time, giving its tighter width. We also observe that the width of the EB CS approaches that of the asymptotic CS as time progresses ($t \geq 10^3$), matching our intuition that the asymptotic variant is a “limit” of our CS (which is also nonasymptotically valid). Finally, we see that the Hoeffding CS is much wider than the EB CS in the first and third cases, but not in the second case where Δ_t has sharp changepoints and the EB CS is wider. We suspect that this happens because the sharp changepoints contribute to having larger values of the intrinsic time \hat{V}_t for the EB CS, whereas the Hoeffding CS simply uses $\hat{V}_t = t$ irrespective of the variance process. Nevertheless, the widths of both CSs eventually reach the “limit” of the asymptotic CS, as t grows large.

In Figure 4, we now plot all pairwise comparisons between the constant baseline (`always_0.5`), the Laplace forecaster (`laplace`), and the K29 forecasters with the 3-degree polynomial kernel and the Gaussian RBF kernel with $\sigma = 0.01$ (`k29_poly3` and `k29_rbf0.01`, respectively). Overall, we find that the K29 forecasters all outperform the Laplace forecaster and the constant baseline, consistently across time. The Laplace forecaster and the constant baseline are also found to be no better than each other, as expected in this synthetic dataset. Between the two K29 forecasters, the ones using the the 3-degree polynomial kernel eventually outperforms the one using the RBF kernel with $\sigma = 0.01$.

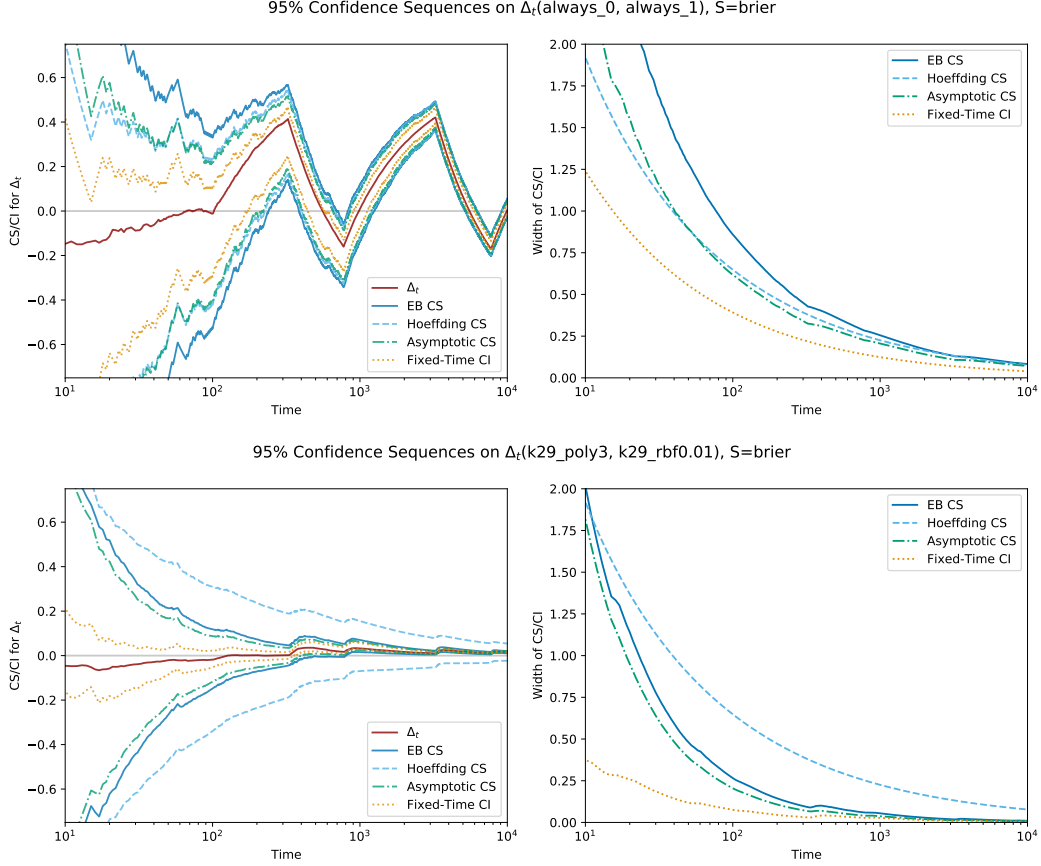


Figure 3: 95% EB CS (blue), Hoeffding-style CS (skyblue, dashed), asymptotic CS (green, dashdot), and fixed-time asymptotic CI (orange, dotted) for Δ_t (left), along with their widths (right), plotted for two additional pairs of forecasts to those in Figure 1. Scoring rule is the Brier score, and positive values of Δ_t indicate that the first forecaster is better than the second. Overall, the asymptotic CS is the tightest CS, followed by the EB CS and the Hoeffding CS. All three CSs cover Δ_t uniformly, and the width of the EB CS approaches that of the asymptotic CS as time grows large. The fixed-time CI is tighter than the CSs, but it does not have a stopping time guarantee. See text for further details.

95% Confidence Sequences on Δ_t , S=brier

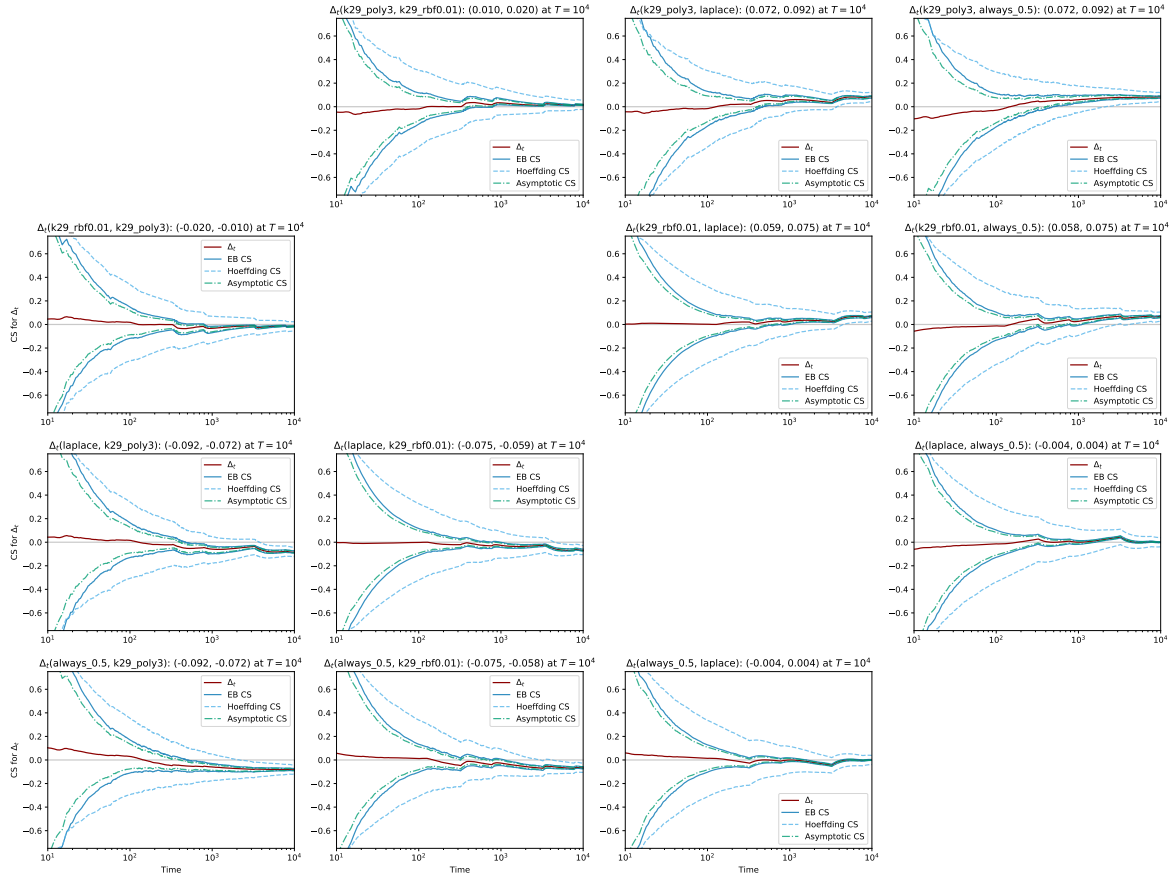


Figure 4: 95% confidence sequences on Δ_t between the constant baseline (`always_0.5`), the Laplace forecaster (`laplace`), and the K29 forecasters with different kernel functions (`k29_poly3` and `k29_rbf0.01`). Scoring rule is the Brier score, and positive values of Δ_t indicate that the first forecaster is better than the second. As before, all three CSs cover Δ_t uniformly, and the width of the EB CS approaches that of the asymptotic CS as time grows large.

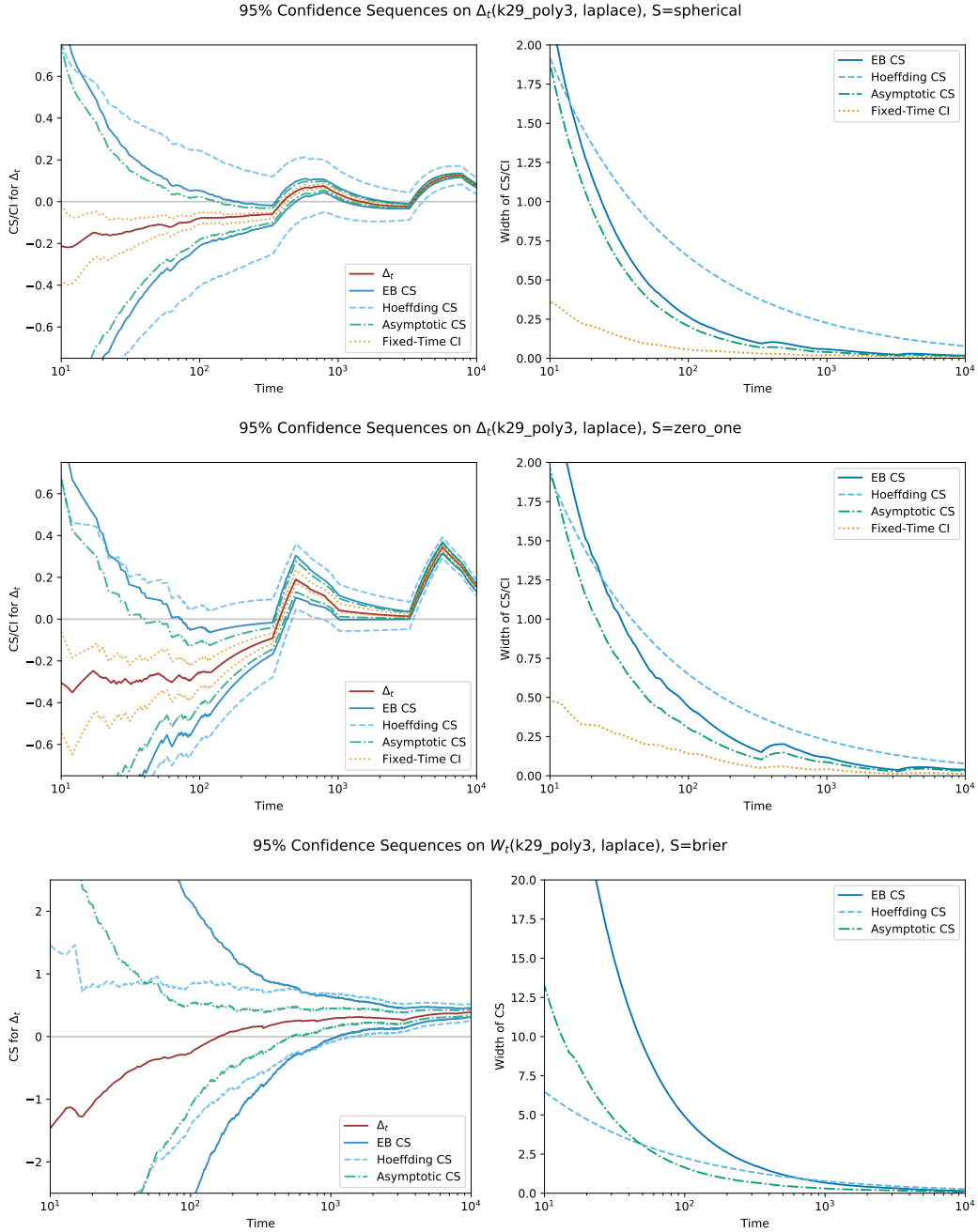


Figure 5: Comparing the use of different scoring rules on simulated data. Top and middle plots show the 95% CS on Δ_t between the K29 forecaster and the Laplace forecaster, using the spherical score and the zero-one score, respectively. Bottom plot shows the 95% CS on Winkler's score W_t of the K29 forecaster against the Laplace forecaster, truncated within values (0.1, 0.9). All scoring rules are defined to be positively oriented, such that positive values of Δ_t or W_t indicate that the first forecaster is better than the second. As in the case of the Brier score, all three CSs cover Δ_t uniformly, and the width of the EB CS approaches that of the asymptotic CS as time grows large.

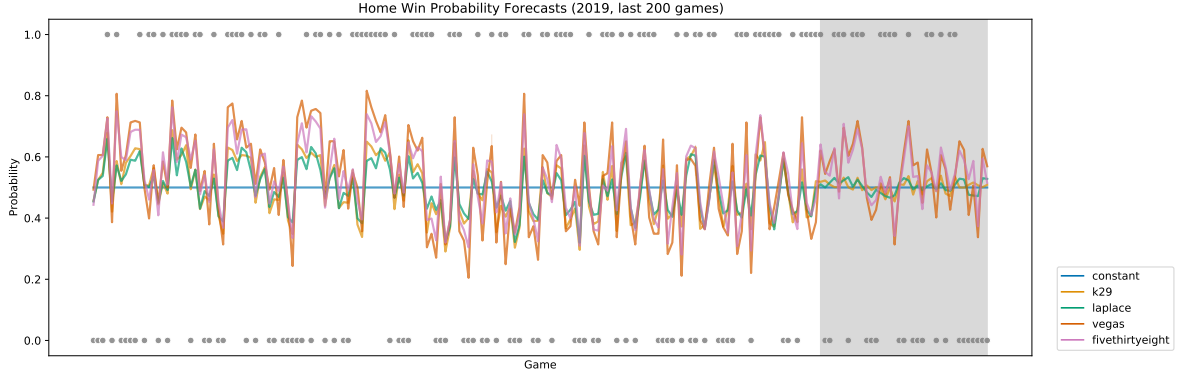


Figure 6: Various forecasters on the last 200 MLB games played in 2019 (including regular season and postseason). FiveThirtyEight and Vegas forecasts are publicly available forecasts online; Laplace and K29 forecasts are made using the historical outcomes as data without external information. *Note that the forecasts are computed using data from a 10-year window (2010 to 2019), but we only show the last year here for visualization purposes.* The shaded region highlights the playoffs (last seven being the World Series games).

Finally, in Figure 5, we plot the 95% CS for comparing the `k29_poly3` forecaster against the Laplace baseline, using the spherical score, the zero-one score, and the Winkler score (with the Brier score). Recall that the spherical score and the zero-one score are bounded and trivially have their linear equivalents, such that Lemma 1 holds, while the pointwise Winkler score satisfies the conditions of Lemma 4. For the average Winkler score, we additionally truncate the Laplace baseline into range $(0.1, 0.9)$ and use the bound $[1 - \frac{2}{0.1}, 1]$ on the pointwise Winkler scores. We observe that the 95% CS always covers the true Δ_t (or W_t) over time, and its width decreases similarly to the case of Brier scores and eventually approaches that of the asymptotic CS. These results illustrate that our CS can also be applied as long as one chooses a scoring rule that has a linear equivalent and has its score differentials bounded.

5.2 Comparing Forecasters on Major League Baseball Games

As our first real-world application of the CSs, we consider the problem of predicting wins and losses for baseball games played in the Major League Baseball (MLB). Sports game prediction is particularly suitable for our setting, because there are multiple publicly available probability forecasts on the outcome of each game (e.g., FiveThirtyEight, betting odds, and pundits/experts), that are frequently updated across time. There is also no obvious assumption to be reasonably made about the outcome of the games, such as stationarity or assumptions of parametric models. Recall Table 1 for an illustration of forecasts made on MLB games.

We specifically focus on predicting the outcome of MLB games, recorded over ten years (2010-2019) culminating in the 2019 World Series between the Houston Astros and the Washington Nationals. We use every regular season and postseason MLB game from 2010 to 2019 as our dataset. We convert each game as a single time point in chronological order, leading to a total of $T = 25,165$ games. As for the forecasters, we consider the following:

- **fivethirtyeight**: Game-by-game probability forecasts on every MLB game since 1871, available on <https://data.fivethirtyeight.com/#mlb-elo>. According to the method-

ology report,¹⁵ the probabilities are calculated using an ELO-based rating system for each team, and game-specific adjustments are made for the starting pitcher as well as other external factors (travel, rest, home field advantage, etc.). Before each new season, team ratings are reverted to the mean by one-third and combined with preseason projections from other sources.¹⁶

- **vegas**: Pre-game closing odds made on each game by online sports bettors, as reported by <https://Vegas-Odds.com>.¹⁷ The betting odds are given in the American format, so each odds o is converted to its implied probability p via $p = \mathbf{1}(o \geq 0) \frac{100}{100+o} + \mathbf{1}(o < 0) \frac{-o}{100-o}$. Then, for each matchup,¹⁸ the pair of implied probabilities for each team is rescaled to sum to 1. For example, given a matchup between team A and team B with betting odds $o_A = -140$ and $o_B = +120$, the implied probabilities are $\tilde{p}_A = 0.58$ and $\tilde{p}_B = 0.45$, and the rescaled probabilities are $p_A = 0.56$ and $p_B = 0.44$.
- **constant**: a constant baseline corresponding to $p_t = 0.5$ for each t .
- **laplace**: A seasonally adjusted Laplace algorithm, representing the season win percentage for each team. Mathematically, it is given by $p_t = \frac{k_t + c_t}{n_t + 1}$, where k_t is the number of wins so far in the season, n_t is the number of games played in this season, and $c_t \in [0, 1]$ is a baseline that represents the final probability forecast from the previous season, reverted to the mean by one-third. For example, if the previous season ended after round t_0 , then $k_t = \sum_{i=t_0}^{t-1} \mathbf{1}(y_i = 1)$, $n_t = t - t_0$, and $c_t = \frac{2}{3} \cdot p_{t_0} + \frac{1}{3} \cdot \frac{1}{2}$ (with $c_0 = \frac{1}{2}$). The final probability forecast for a game between two teams is rescaled to sum to 1.
- **k29**: The K29 algorithm applied to each team, using the Gaussian kernel with $\sigma = 0.1$, computed using data from the current season only. The final probability forecast for a game between two teams is rescaled to sum to 1.

In Figure 6, we plot the five probability forecasters on the last 200 games of 2019.

We perform all pairwise comparisons of the five aforementioned forecasters on the 10-year win/loss predictions. Note that we conduct this experiment as a *post-hoc* analysis, since all games have already been played — the only difference from an online analysis is that we can further optimize our uniform boundary to be the tightest at the final time step ($v_{\text{opt}} = \hat{V}_T$). Importantly, the procedure still takes into account that the games were forecast sequentially, and it still compares the forecasters in terms of their *predictive* performance by estimating $\Delta_t = (1/t) \sum_{i=1}^t \mathbb{E}[S(p_i, y_i) - S(q_i, y_i) | \mathcal{G}_{i-1}]$.

First, we list the 95% EB CS on the average score differential Δ_T as well as the average Winkler score W_T against the **laplace** baseline in Table 4. Our results suggest that the two publicly available forecasters, **fivethirtyeight** and **vegas**, outperform all baselines including the season-adjusted win percentage (**laplace**), both in terms of the Brier score and the Winkler score. This makes intuitive sense, as only the **fivethirtyeight** and **vegas** forecasters use sophisticated forecasting models involving external information about the game (as well as expert opinions). For the baseline models, we find that the **k29** forecaster underperforms **laplace**, suggesting that both the defensive forecaster is worse than the season-adjusted running average. One reason why the **k29** forecaster underperforms **laplace** might be that it

¹⁵<https://fivethirtyeight.com/features/how-our-mlb-predictions-work/>

¹⁶Baseball Prospectus's PECOTA, FanGraphs' depth charts, and Clay Davenport's predictions

¹⁷Download source: <https://sports-statistics.com/sports-data/mlb-historical-odds-scores-datasets/>

¹⁸In any given matchup, the sum of two implied probabilities is typically greater than 1, and the excess reflects the bettor's profit margin (also known as overreach or vigorish).

Forecaster	95% EB CS
<code>fivethirtyeight</code>	(0.00458, 0.00792)
<code>vegas</code>	(0.00600, 0.00977)
<code>k29</code>	(-0.00522, -0.00198)
<code>constant</code>	(-0.00294, 0.00043)

(a) Δ_T (using Brier) against `laplace`

Forecaster	95% EB CS
<code>fivethirtyeight</code>	(0.04927, 0.09669)
<code>vegas</code>	(0.05208, 0.09973)
<code>k29</code>	(-0.09697, -0.04107)
<code>constant</code>	(-0.06718, -0.02380)

(b) W_T against `laplace`

Table 4: 95% EB CS on the average Brier score differential Δ_T and the average Winkler score W_T , against the `laplace` forecaster as a baseline ($T = 25, 165$). Positive (negative) values of Δ_T or W_T indicate that the forecaster is better (worse) than the baseline. We find that both the `fivethirtyeight` and `vegas` forecasters outperform the `laplace` baseline, while the other two baselines perform worse (or no better) than `laplace`.

is more likely to make overconfident (but often incorrect) predictions, which is problematic in predicting outcomes that have high randomness like sports games. We also find that the `constant` forecaster is found to be similar in predictive performance to the `laplace` forecaster in Brier score and worse in Winkler score.

In Figure 7, we now plot the 95% Hoeffding, EB, and asymptotic CSs between all pairs of the five forecasters. We find across pairs that the EB CS is much tighter than the Hoeffding CS and as tight as the asymptotic CS for larger t . In terms of forecaster comparison, we additionally find that the `vegas` forecaster outperforms the `fivethirtyeight` forecaster (95% EB CS for Δ_T is $(-0.00267, -0.00060)$ at $T = 25, 165$), while both forecasters outperform all other baselines (`k29` and `constant`). The fact that the `vegas` forecaster (marginally) outperforms the `fivethirtyeight` forecaster is interesting, especially given that the primary goal of sports bettors is not to maximize predictive accuracy but their overall profit.¹⁹ Yet, given the relatively small score difference and also the inherent uncertainty in sports game outcomes,²⁰ more fine-grained comparisons between real-world sports forecasters (e.g., regular season vs. playoffs, team-specific comparisons, comparisons with or without specific side information, and other sports) would be an interesting future work.

Finally, note that we can re-compute the CSs with a prespecified value of v_{opt} , instead of using $v_{\text{opt}} = \hat{V}_T$, such that they remain valid in the scenario where one starts from $t = 1$ and continuously collect data compare forecasts as time progresses. For example, a statistician who compares `fivethirtyeight` and `laplace` forecasters after each game can decide, after some time τ at which the entire CS falls below zero, that the latter outperforms the former, without having to worry about “sampling to a foregone conclusion” (Anscombe, 1954). The statistician can also use the CSs to find, for instance, that the `vegas` forecaster is better than the `fivethirtyeight` going into Game 7 of the 2019 World Series, by observing that the 95% EB CS for $\Delta_t(\text{vegas}, \text{fivethirtyeight})$ drops entirely below zero after some time, using the stopping rule (19).

¹⁹<https://fivethirtyeight.com/features/the-imperfect-pursuit-of-a-perfect-baseball-forecast/>

²⁰<https://projects.fivethirtyeight.com/checking-our-work/mlb-games/>

95% Confidence Sequences on Δ_t , $S=\text{brier}$

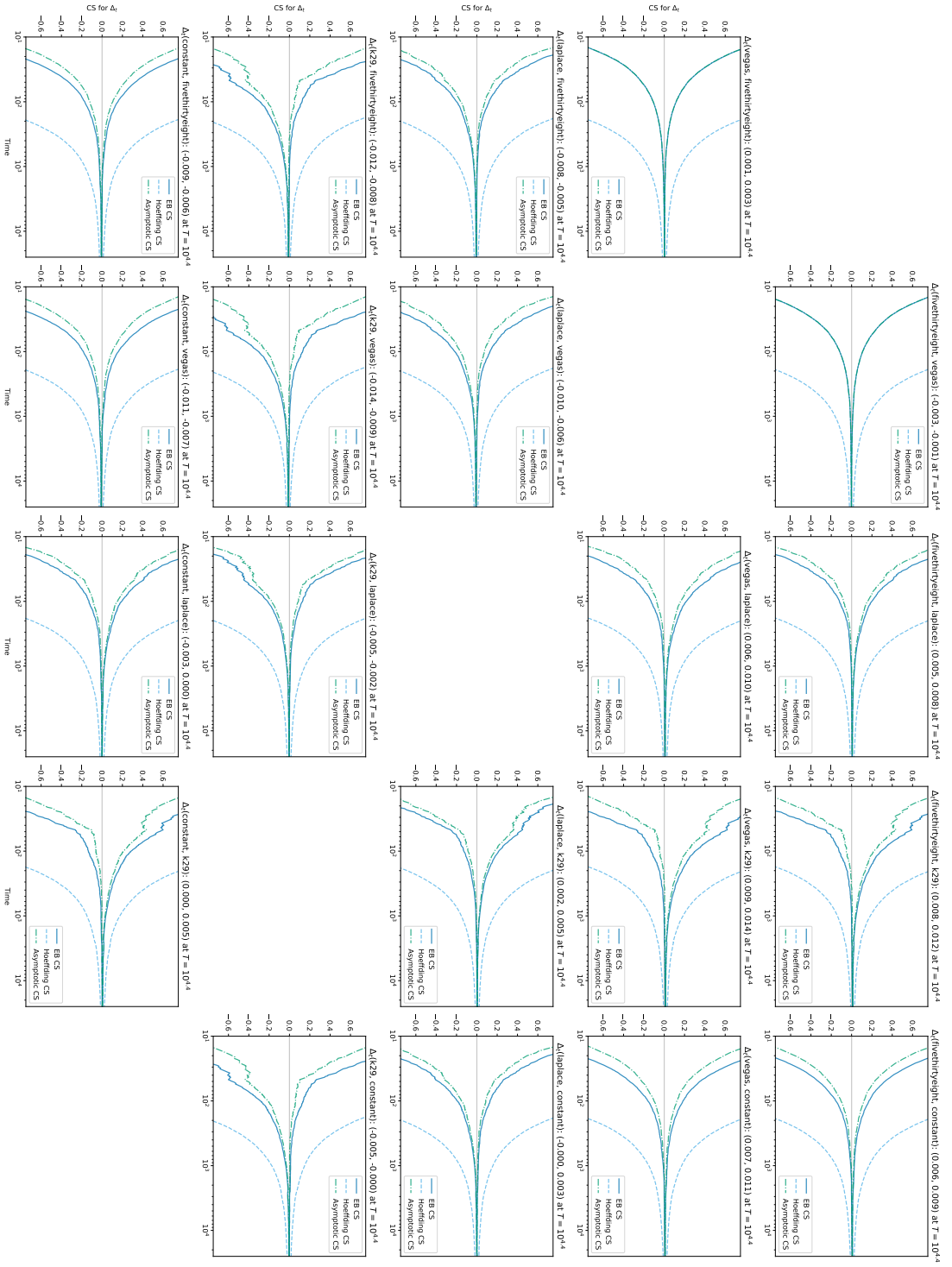


Figure 7: Comparing MLB win probability forecasts from 2010 to 2019, using our CSs as well as the asymptotic CS at significance level $\alpha = 0.05$. $T = 25, 165 \approx 10^{4.4}$ corresponds to the final game of the 2019 World Series. Note that the horizontal axis is drawn in log-scale. The Brier score is used. We find that, over time, the five forecasters are found to achieve significantly different predictive performance from each other (except `laplace` and `constant`), with the `vegas` forecaster achieving the best performance, followed by `fivethirtyeight`, `laplace` \approx `constant`, and `k29`. See title of each subplot for the 95% EB CS at $T = 25, 165$.

5.3 Comparing Statistical Postprocessing Methods for Weather Forecasts

As our second real-data experiment and an illustration of our e-processes derived in Section 3.5, we compare a set of statistical postprocessing methods for weather forecasts (Vannitsem et al., 2021), following recent work by Henzi and Ziegel (2021). Statistical postprocessing here refers to the process of correcting for biases and dispersion errors in ensemble weather forecasts, which are produced by perturbing the initial conditions of numerical weather prediction (NWP) methods. As ensemble forecasts are commonly used in state-of-the-art weather forecasting systems as a means of producing probabilistic forecasts, statistical postprocessing is considered a key component of modern weather forecasting.

In their work, Henzi and Ziegel (2021) compare statistical postprocessing methods for predicting the Probability of Precipitation (PoP) using the ensemble forecast data from the European Centre for Medium-Range Weather Forecasts (ECMWF; Molteni et al. (1996)). The dataset includes the observed 24-hour precipitation from January 06, 2007 to January 01, 2017 at four airport locations (Brussels, Frankfurt, London Heathrow, and Zurich), and for each location and date it also includes 1- to 5-day ensemble forecasts, consisting of a high resolution forecast, 50 perturbed ensemble forecasts at a lower resolution, and a control run for the perturbed forecasts. They consider three statistical postprocessing methods in their experiments: isotonic distributional regression (IDR; Henzi et al. (2021)) and heteroscedastic censored logistic regression (HCLR; Messner et al. (2014)), as well as a variant of HCLR without its scale parameter (HCLR_). Each method is applied to the first-half of the data, separately for each airport location and lag $h = 1, \dots, 5$, and the second-half data is used to make sequential comparisons of the postprocessing methods. Note that each location has a different number of observations: 3,406 for Brussels, 3,617 for Frankfurt, 2,256 for London, and 3,241 for Frankfurt. See Section 5 in Henzi et al. (2021) and Section 5.1 in Henzi and Ziegel (2021) for further details about the dataset and the postprocessing methods. In Figure 8, we plot the three postprocessing methods for 1-day PoP forecasts for one of the airport locations (Brussels) in the final year (January 01, 2016 to January 01, 2017).

Our main goal here is to sequentially compare the three statistical postprocessing methods using our EB CS from Theorem 2. As noted in Sections 1.1 and 3.5, the inferential conclusions drawn from our CS are different than those from Henzi and Ziegel (2021), who provide a test of *step-by-step* conditional forecast dominance instead of *average*. While rejecting the null in the e-value-based sequential test only tells us that there exists some time point where one forecaster outperforms another, finding that our CS for the average score differentials is away from zero tells us that one forecaster tends to outperform another in predicting the next outcome. As such, if we were to convert our CS into its corresponding sequential test, we would expect our version to have a larger null set and thus reject less the null often. On the other hand, the two methods are similar in that they both come with anytime-valid guarantees, in particular at arbitrary stopping times, such that one can “safely” (Johari et al., 2015; Grünwald et al., 2019) update their conclusions as more data is collected.

In Figure 9, we plot both the 90% EB CS on Δ_t (top) as well as the corresponding sub-exponential e-values for the weak one-sided null H_0^w (bottom), between HCLR and IDR, IDR and HCLR_, and HCLR and HCLR_ on 1-day PoP forecasts, using the Brier score. Note that these are the same three pairs compared in Figure 3 of Henzi and Ziegel (2021), which would correspond to e-values for the strong one-sided null H_0^s . The EB CS is computed using Theorem 2 and the gamma-exponential CM boundary from Lemma 2; the e-values are then computed using Theorem 3 and the exponential supermartingale that constructs the gamma-exponential CM boundary for the CS, as described in Section 3.5. We use the same

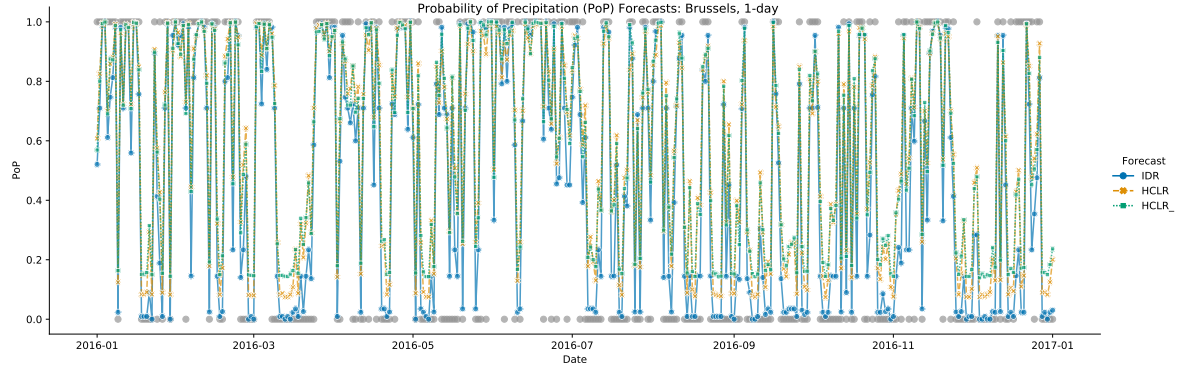


Figure 8: Comparing three statistical postprocessing methods (IDR, HCLR, HCLR₊) for ensemble weather forecasts on the Probability of Precipitation (PoP). The binary outcome is drawn as gray dots. For visualization purposes, we plot the data and the forecasts only for the final year (January 01, 2016 to January 01, 2017) and at one airport location (Brussels) with lag 1.

set of hyperparameters ($c = 0.1$, $v_{\text{opt}} = 0.5$, and $\rho = \frac{v_{\text{opt}}}{W_{-1}(\alpha^2/e)+1}$ with $\alpha = 0.1$, following Proposition 3(a) in [Howard et al. \(2021\)](#)) for both the CS and the e-values, as they rely on the same underlying supermartingale. Here we choose the significance level of $\alpha = 0.1$, because it roughly corresponds to the threshold of 10 for e-values to be considered a “strong” evidence against the null ([Vovk and Wang, 2021](#)).

We first note from Figure 9 that the lower bound of our 90% EB CSs on $\Delta_t(p, q)$ and the e-values for $H_0^W : \Delta_t(p, q) \leq 0$ share a similar trend over time, where e-values grow large when the lower bound grows significantly larger than zero, implying that the forecaster p is better than the forecaster q , following (19). Whereas the CSs provide a (two-sided) estimate of $\Delta_t(p, q)$ with uncertainty, the e-values explicitly give the amount of evidence for whether one is better than the other. In this way, the two procedures complement each other for the purpose of sequentially valid inference on Δ_t . We finally note that, while the e-values are defined for one-sided nulls on $\Delta_t(p, q)$, we can also compute the e-values for $H_0^W : \Delta_t(q, p) \leq 0$, and they would correspond to the upper bound of the EB CSs.

In terms of the inferential conclusions based on 1-day forecasts, we find from the 90% CSs that IDR forecasts are found to outperform both HCLR and HCLR₊ 1-day forecasts for Brussels, and that HCLR forecasts outperform HCLR₊ forecasts for Frankfurt and Zurich, but we do not find significant differences at other locations between other pairs. Our e-values (with a threshold at 10) also lead to the same conclusions, and they also more clearly visualize at which point in time is one forecaster first found to outperform the other and how that pattern changes (e.g., when comparing IDR to HCLR₊ for Brussels, IDR is found to be better as early as 2012, and it also shows the period between late 2012 and late 2015 where it is no longer found to be better, before eventually regaining evidence favoring IDR starting 2016).

When we compare our e-values for the weak null H_0^W with the e-values for the strong null H_0^S provided by [Henzi and Ziegel \(2021\)](#) (Figure 3), we find that e-values for the strong null are large whenever e-values for the weak null are also large, but not vice versa. Specifically, the comparisons of IDR against HCLR₊ and HCLR against HCLR₊ in Frankfurt are only found to have strong evidence against the strong null, but not the weak null. This is consistent with our previous discussion in Section 3.5 that the strong null implies the weak null and thus is easier to “reject” (or gather more evidence against), although rejecting the weak null is more

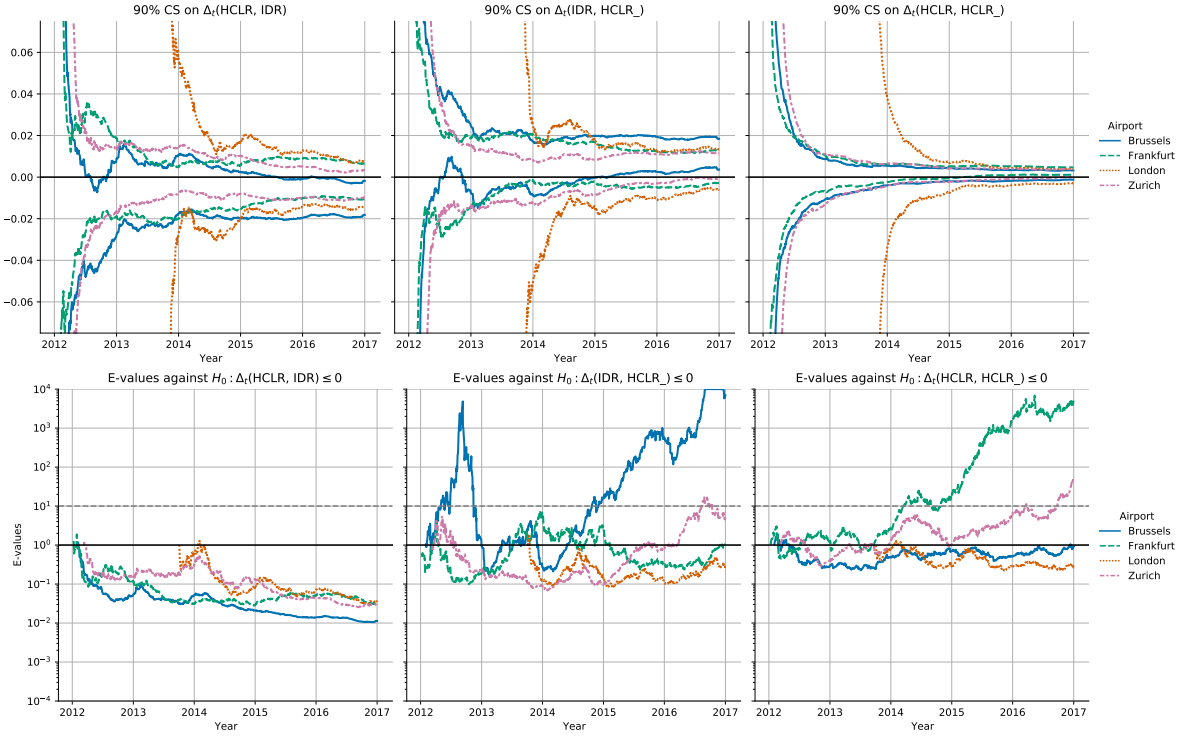


Figure 9: (Top) 90% EB CSs for Δ_t between pairs of statistical postprocessing methods (HCLR and IDR; IDR and HCLR_{_}; HCLR and HCLR_{_}) for 1-day ensemble forecasts using Theorem 2, computed and plotted separately for each airport: Brussels ($T = 1,703$), Frankfurt ($T = 1,809$), London ($T = 1,128$), and Zurich ($T = 1,621$). Note that positive/negative scores of $\Delta_t(\mathbf{p}, \mathbf{q})$ indicates that forecaster \mathbf{p} is better/worse than forecaster \mathbf{q} . Overall, the CSs capture the time-varying score gap on average between the two forecasters across the years. (Bottom) E-values for the null that $H_0^W : \Delta_t \leq 0$, corresponding to (the lower bound of) the 90% CSs above. These e-values are the *weak* or *average* counterpart to [Henzi and Ziegel \(2021\)](#)'s e-values for the *strong* or *step-by-step* null that $H_0^S : \delta_i \leq 0 \forall i = 1, \dots, t$. Note that the e-values exceed 10 approximately when the lower bound of the 90% CS exceeds 0. Both procedures use the Brier score as the scoring rule. See text for further details.

informative as it provides a cumulative comparison over time. For example, in Frankfurt, we can infer we only have strong evidence that IDR has outperformed HCLR_{_} *at some point in time* between 2012 and 2017, but we do not have sufficient evidence that IDR has outperformed HCLR_{_} *on a typical day* in the same time period.

In Table 5, we further compare the e-values for the weak null (E^W) and the strong null (E^S), evaluated at the last time step T (January 01, 2017) for each location and lag ($1, \dots, 5$), where T corresponds to January 01, 2017. Here, we also find that e-values for the weak null are large mostly when e-values for the strong null are large. Using an e-value threshold of 10, there are a total of 22 out of 60 comparisons where E^S is large, compared to only 16 for E^W . The conclusions overlap for 11 comparisons, and all 5 comparisons for which only E^W exceeds 10 are those between HCLR and HCLR_{_}, suggesting that HCLR forecasts seem to perform better than HCLR_{_} when compared using the average score differentials. Conversely, 9 out of 11 comparisons for which only E^S exceeds 10 are those between IDR and HCLR_{_}, suggesting that there is less evidence that HCLR_{_} outperforms IDR when compared using the average

Location	Lag	HCLR/IDR		IDR/HCLR		HCLR/HCLR	
		E^w	E^s	E^w	E^s	E^w	E^s
Brussels	1	0.011	0	> 100	> 100	0.915	> 100
	2	0.021	0.01	2.426	> 100	1.871	13.602
	3	0.056	0.425	0.142	> 100	15.606	15.185
	4	1.307	4.804	0.021	1.943	4.078	5.165
	5	58.929	16.969	0.015	0.415	54.825	3.436
Frankfurt	1	0.031	0	1.079	> 100	> 100	> 100
	2	0.020	0.054	71.817	> 100	> 100	> 100
	3	0.021	0.078	> 100	> 100	> 100	26.569
	4	0.297	2.291	0.065	9.618	> 100	5.54
	5	0.829	1.526	0.029	2.362	8.285	3.227
London	1	0.037	0.029	0.247	14.979	0.262	2.845
	2	0.028	0.188	0.625	> 100	0.184	2.868
	3	0.043	0.734	0.262	40.905	0.228	2.488
	4	0.141	1.429	0.076	1.7	0.753	1.744
	5	0.375	1.577	0.034	0.379	0.249	1.118
Zurich	1	0.031	0.003	4.973	> 100	56.612	61.747
	2	0.049	0.116	0.903	36.891	> 100	10.276
	3	0.301	1.516	0.091	31.924	> 100	5.098
	4	3.788	4.069	0.031	1.276	18.219	2.771
	5	> 100	15.151	0.021	0.842	> 100	2.383

Table 5: E-values between pairs of statistical postprocessing methods for ensemble weather forecasts across different locations and lags, where T is the last time step (January 01, 2017). E^w indicates e-values for the weak null $H_0^w(p, q) : \Delta_t(p, q) \leq 0$, computed using Theorem 3; E^s indicates e-values for the strong null $H_0^s(p, q) : \delta_i(p, q) \leq 0 \forall i = 1, \dots, t$, computed by [Henzi and Ziegel \(2021\)](#). Both procedures use the Brier score as the scoring rule. “q/p” indicates CS on $\Delta_T(p, q)$. Across different locations and lags, E^s is large (greater than 10) at 22 location-lag pairs, compared to 16 for E^w (11 of which overlap). See text for further details.

score differentials (for E^w). Together, we see that E^w gives less evidence than E^s that HCLR $_-$ can perform as well as or better than IDR or HCLR. Finally, we also include the 90% EB CSs on Δ_T in Table 6, which is consistent with the e-values for the weak null in Table 5 but further provides a symmetric comparison between pairs of forecasters.

6 Conclusions

In this work, we derived time-uniform CSs that allow us to sequentially compare the quality of probability forecasts at arbitrary stopping times. These CSs require no distributional assumptions on the sequence of outcomes, such as stationarity, or on how the forecasts are generated. We also derived e-processes and anytime-valid p-processes that correspond to our CSs, and also discussed several extensions of our CSs, including forecasts on categorical outcomes, k -step-ahead forecasts, mean forecasts on sub-Gaussian continuous outcomes, and Winkler’s normalized score. We’ve empirically illustrated the validity of the CSs on synthetic data and showed their applications to real-world baseball forecasts and weather forecasts. In doing so, we also provided comparisons with fixed-time CIs ([Lai et al., 2011](#)) that are invalid at stopping

Location	Lag	HCLR/IDR	IDR/HCLR	HCLR/HCLR
Brussels	1	(-0.018, -0.002)	(0.004, 0.018)	(-0.001, 0.003)
	2	(-0.013, 0.004)	(-0.002, 0.014)	(-0.001, 0.004)
	3	(-0.010, 0.011)	(-0.006, 0.012)	(-0.000, 0.006)
	4	(-0.003, 0.017)	(-0.014, 0.005)	(-0.001, 0.006)
	5	(0.001, 0.019)	(-0.016, 0.001)	(0.000, 0.006)
Frankfurt	1	(-0.011, 0.006)	(-0.003, 0.013)	(0.001, 0.005)
	2	(-0.013, 0.003)	(0.001, 0.015)	(0.001, 0.006)
	3	(-0.013, 0.004)	(0.001, 0.016)	(0.002, 0.007)
	4	(-0.004, 0.011)	(-0.007, 0.007)	(0.001, 0.006)
	5	(-0.003, 0.013)	(-0.010, 0.004)	(-0.000, 0.005)
London	1	(-0.014, 0.008)	(-0.006, 0.013)	(-0.003, 0.004)
	2	(-0.016, 0.006)	(-0.004, 0.015)	(-0.004, 0.005)
	3	(-0.013, 0.008)	(-0.006, 0.012)	(-0.004, 0.005)
	4	(-0.008, 0.013)	(-0.009, 0.008)	(-0.002, 0.007)
	5	(-0.006, 0.016)	(-0.013, 0.005)	(-0.004, 0.005)
Zurich	1	(-0.010, 0.003)	(-0.001, 0.011)	(0.000, 0.004)
	2	(-0.008, 0.006)	(-0.003, 0.010)	(0.001, 0.004)
	3	(-0.004, 0.010)	(-0.006, 0.007)	(0.001, 0.005)
	4	(-0.001, 0.012)	(-0.010, 0.003)	(-0.000, 0.005)
	5	(0.002, 0.015)	(-0.011, 0.000)	(0.001, 0.006)

Table 6: 90% EB CS on Δ_T between pairs of statistical postprocessing methods for ensemble weather forecasts across different locations and lags, where T is the last time step (January 01, 2017). “q/p” indicates CS on $\Delta_T(p, q)$. We use the Brier score as the scoring rule. Note that positive values of $\Delta_T(p, q)$ indicates that p outperforms q . The CSs give estimates of $\Delta_T(p, q)$ with uncertainty, and they provide a symmetric comparison of the forecasters unlike the e-values.

times and cannot be sequentially tracked, as well as more recent e-values that were developed for a strong null (Henzi and Ziegel, 2021), rather than our more preferable weak null.

Acknowledgements

AR acknowledges funding from NSF DMS 1916320. Research reported in this paper was sponsored in part by the DEVCOM Army Research Laboratory under Cooperative Agreement W911NF-17-2-0196 (ARL IoT CRA). The views and conclusions contained in this document are those of the authors and should not be interpreted as representing the official policies, either expressed or implied, of the Army Research Laboratory or the U.S. Government. The U.S. Government is authorized to reproduce and distribute reprints for Government purposes notwithstanding any copyright notation herein. YJC and AR thank Ruodu Wang and Glenn Shafer, who were coinstructors with AR on a tri-university game-theoretic statistical inference course, for which this paper started off as a course project.

References

Anscombe, F. J. (1954). Fixed-sample-size analysis of sequential observations. *Biometrics*, 10(1):89–100.

Brier, G. W. (1950). Verification of forecasts expressed in terms of probability. *Monthly weather review*, 78(1):1–3.

Darling, D. A. and Robbins, H. (1967). Confidence sequences for mean, variance, and median. *Proceedings of the National Academy of Sciences of the United States of America*, 58(1):66.

Dawid, A. P. (1984). Statistical theory: the prequential approach. *Journal of the Royal Statistical Society: Series A (General)*, 147(2):278–290.

DeGroot, M. H. and Fienberg, S. E. (1983). The comparison and evaluation of forecasters. *Journal of the Royal Statistical Society: Series D (The Statistician)*, 32(1-2):12–22.

Diebold, F. X. and Mariano, R. S. (1995). Comparing predictive accuracy. *Journal of Business & Economic Statistics*, 13(3).

Doob, J. L. (1940). Regularity properties of certain families of chance variables. *Transactions of the American Mathematical Society*, 47(3):455–486.

Ehm, W. and Krüger, F. (2018). Forecast dominance testing via sign randomization. *Electronic Journal of Statistics*, 12(2):3758–3793.

Fan, X., Grama, I., and Liu, Q. (2015). Exponential inequalities for martingales with applications. *Electronic Journal of Probability*, 20.

Garthwaite, P. H., Kadane, J. B., and O'Hagan, A. (2005). Statistical methods for eliciting probability distributions. *Journal of the American Statistical Association*, 100(470):680–701.

Giacomini, R. and White, H. (2006). Tests of conditional predictive ability. *Econometrica*, 74(6):1545–1578.

Gneiting, T. (2011). Making and evaluating point forecasts. *Journal of the American Statistical Association*, 106(494):746–762.

Gneiting, T., Balabdaoui, F., and Raftery, A. E. (2007). Probabilistic forecasts, calibration and sharpness. *Journal of the Royal Statistical Society: Series B (Statistical Methodology)*, 69(2):243–268.

Gneiting, T. and Katzfuss, M. (2014). Probabilistic forecasting. *Annual Review of Statistics and Its Application*, 1(1):125–151.

Gneiting, T. and Raftery, A. E. (2007). Strictly proper scoring rules, prediction, and estimation. *Journal of the American statistical Association*, 102(477):359–378.

Good, I. (1971). Comment on “Measuring information and uncertainty” by Robert J. Buehler. *Foundations of Statistical Inference*, pages 337–339.

Good, I. J. (1952). Rational decisions. *Journal of the Royal Statistical Society: Series B (Methodological)*, 14(1):107–114.

Grünwald, P., de Heide, R., and Koolen, W. (2019). Safe testing. *arXiv preprint arXiv:1906.07801*.

Henzi, A. and Ziegel, J. F. (2021). Valid sequential inference on probability forecast performance. *arXiv preprint arXiv:2103.08402*.

Henzi, A., Ziegel, J. F., and Gneiting, T. (2021). Isotonic distributional regression. *Journal of the Royal Statistical Society: Series B (Statistical Methodology)*.

Hoeffding, W. (1963). Probability inequalities for sums of bounded random variables. *Journal of the American Statistical Association*, 58(301):13–30.

Howard, S. R., Ramdas, A., McAuliffe, J., and Sekhon, J. (2020). Time-uniform chernoff bounds via nonnegative supermartingales. *Probability Surveys*, 17:257–317.

Howard, S. R., Ramdas, A., McAuliffe, J., and Sekhon, J. (2021). Time-uniform, nonparametric, nonasymptotic confidence sequences. *The Annals of Statistics*, 49(2):1055 – 1080.

Jamieson, K. and Jain, L. (2018). A bandit approach to multiple testing with false discovery control. In *Proceedings of the 32nd International Conference on Neural Information Processing Systems*, pages 3664–3674.

Jamieson, K., Malloy, M., Nowak, R., and Bubeck, S. (2014). lil’UCB: An optimal exploration algorithm for multi-armed bandits. In *Conference on Learning Theory*, pages 423–439. PMLR.

Johari, R., Pekelis, L., and Walsh, D. J. (2015). Always valid inference: Bringing sequential analysis to A/B testing. *arXiv preprint arXiv:1512.04922*.

Karampatziakis, N., Mineiro, P., and Ramdas, A. (2021). Off-policy confidence sequences. In Meila, M. and Zhang, T., editors, *Proceedings of the 38th International Conference on Machine Learning*, volume 139 of *Proceedings of Machine Learning Research*, pages 5301–5310. PMLR.

Lai, T. L. (1976a). Boundary crossing probabilities for sample sums and confidence sequences. *The Annals of Probability*, pages 299–312.

Lai, T. L. (1976b). On confidence sequences. *The Annals of Statistics*, 4(2):265–280.

Lai, T. L., Gross, S. T., and Shen, D. B. (2011). Evaluating probability forecasts. *The Annals of Statistics*, 39(5):2356–2382.

Lehmann, E. L. (1975). *Nonparametrics: statistical methods based on ranks*. Holden-day.

Messner, J. W., Mayr, G. J., Wilks, D. S., and Zeileis, A. (2014). Extending extended logistic regression: Extended versus separate versus ordered versus censored. *Monthly Weather Review*, 142(8):3003–3014.

Molteni, F., Buizza, R., Palmer, T. N., and Petroliagis, T. (1996). The ECMWF ensemble prediction system: Methodology and validation. *Quarterly journal of the royal meteorological society*, 122(529):73–119.

Ramdas, A., Ruf, J., Larsson, M., and Koolen, W. (2020). Admissible anytime-valid sequential inference must rely on nonnegative martingales. *arXiv preprint arXiv:2009.03167*.

Ramdas, A., Ruf, J., Larsson, M., and Koolen, W. M. (2021). Testing exchangeability: Fork-convexity, supermartingales and e-processes. *International Journal of Approximate Reasoning*.

Robbins, H. (1970). Statistical methods related to the law of the iterated logarithm. *The Annals of Mathematical Statistics*, 41(5):1397–1409.

Robbins, H. and Siegmund, D. (1970). Boundary crossing probabilities for the wiener process and sample sums. *The Annals of Mathematical Statistics*, pages 1410–1429.

Rosenbaum, P. R. (1995). *Observational studies*. Springer.

Schervish, M. J. (1989). A general method for comparing probability assessors. *The Annals of Statistics*, 17(4):1856 – 1879.

Shafer, G. (2021). Testing by betting: A strategy for statistical and scientific communication. *Journal of the Royal Statistical Society: Series A (Statistics in Society)*, 184(2):407–431.

Shafer, G. and Vovk, V. (2019). *Game-Theoretic Foundations for Probability and Finance*, volume 455. John Wiley & Sons.

Vannitsem, S., Bremnes, J. B., Demaeyer, J., Evans, G. R., Flowerdew, J., Hemri, S., Lerch, S., Roberts, N., Theis, S., and Atencia, A. (2021). Statistical postprocessing for weather forecasts: Review, challenges, and avenues in a big data world. *Bulletin of the American Meteorological Society*, 102(3):E681–E699.

Ville, J. (1939). Etude critique de la notion de collectif. *Bull. Amer. Math. Soc*, 45(11):824.

Vovk, V., Takemura, A., and Shafer, G. (2005). Defensive forecasting. In *International Workshop on Artificial Intelligence and Statistics*, pages 365–372. PMLR.

Vovk, V. and Wang, R. (2021). E-values: Calibration, combination and applications. *The Annals of Statistics*, 49(3):1736 – 1754.

Wainwright, M. J. (2019). *High-dimensional statistics: A non-asymptotic viewpoint*, volume 48. Cambridge University Press.

Waudby-Smith, I., Arbour, D., Sinha, R., Kennedy, E. H., and Ramdas, A. (2021). Doubly robust confidence sequences for sequential causal inference. *arXiv preprint arXiv:2103.06476*.

Waudby-Smith, I. and Ramdas, A. (2020). Estimating means of bounded random variables by betting. *arXiv preprint arXiv:2010.09686*.

Winkler, R. L. (1994). Evaluating probabilities: Asymmetric scoring rules. *Management Science*, 40(11):1395–1405.

Winkler, R. L., Munoz, J., Cervera, J. L., Bernardo, J. M., Blattenberger, G., Kadane, J. B., Lindley, D. V., Murphy, A. H., Oliver, R. M., and Ríos-Insua, D. (1996). Scoring rules and the evaluation of probabilities. *Test*, 5(1):1–60.

Wu, J. and Ding, P. (2020). Randomization tests for weak null hypotheses in randomized experiments. *Journal of the American Statistical Association*, pages 1–16.

Zhao, S., Zhou, E., Sabharwal, A., and Ermon, S. (2016). Adaptive concentration inequalities for sequential decision problems. *Advances in Neural Information Processing Systems*, 29:1343–1351.

A Tight Confidence Sequences via Uniform Boundaries

The confidence sequences we derive in this work rely on the tight CSs derived in Howard et al. (2021) using the technique of time-uniform Chernoff bounds via uniform boundaries (Howard et al., 2020). Here, we briefly summarize the key definitions required for deriving our CSs.

Let $(S_t)_{t=0}^\infty, (V_t)_{t=0}^\infty$ be real-valued processes adapted to a filtration $(\mathcal{G}_t)_{t=0}^\infty$, with $S_0 = V_0 = 0$ and $V_t \geq 0$ for all t . S_t can be thought of as a summary statistic accumulated up to time t , such as $\bar{X}_t = \sum_{i=1}^t X_i$, and $(V_t)_{t=0}^\infty$ as an intrinsic time measured by the variance accumulated up to time t . Further, let $\psi : [0, \lambda_{\max}] \rightarrow \mathbb{R}$ be a cumulant generative function (CGF) of a random variable, such as a standard Gaussian, an exponential, or a gamma. A working example throughout the paper is the exponential CGF: $\psi_{E,c}(\lambda) = c^{-2}(-\log(1 - c\lambda) - c\lambda)$ for $c > 0$. We denote $\psi_E = \psi_{E,1}$.

We say that $(S_t)_{t=0}^\infty$ is *sub- ψ with variance process* $(V_t)_{t=0}^\infty$ if, for each $\lambda \in [0, \lambda_{\max}]$, there exists a supermartingale $(L_t(\lambda))_{t=0}^\infty$ with respect to $(\mathcal{G}_t)_{t=0}^\infty$ such that $\mathbb{E}[L_0(\lambda)] \leq 1$ and

$$\exp\{\lambda S_t - \psi(\lambda)V_t\} \leq L_t(\lambda) \text{ a.s. for all } t. \quad (36)$$

Let $\mathbb{S}_\psi = \{((S_t, V_t))_{t=0}^\infty : (S_t)_{t=0}^\infty \text{ is sub-}\psi \text{ with variance process } (V_t)_{t=0}^\infty\}$. Then, a function $u : \mathbb{R} \rightarrow \mathbb{R}$ is a *sub- ψ uniform boundary with crossing probability* $\alpha \in (0, 1)$ *for scale* $c \in \mathbb{R}$ if

$$\sup_{(S_t, V_t) \in \mathbb{S}_\psi} \mathbb{P}(\exists t \geq 1 : S_t \geq u(V_t)) \leq \alpha. \quad (37)$$

These uniform boundaries based on exponential supermartingales provide time-uniform and non-asymptotic bounds for summary statistics regardless of the underlying distributional assumptions. In this work, we will utilize sub-exponential uniform boundaries, i.e., sub- ψ uniform boundaries with $\psi_{E,c}(\lambda) = c^{-2}(-\log(1 - c\lambda) - \lambda)$ for some $c \in \mathbb{R}$, that are used to derive tight confidence sequences in Howard et al. (2021).

B Proofs

B.1 Proof of Lemma 1

The definition of linear equivalents and this (simple) lemma are due to Lai et al. (2011). Let \tilde{S} be a linear equivalent of S . By its linearity on its second argument and by (5), we have that, for each i ,

$$\mathbb{E}\left[\tilde{S}(p_i, y_i) \mid \mathcal{G}_{i-1}\right] = \tilde{S}(p_i, r_i). \quad (38)$$

Also, let $d(r) := S(p, r) - \tilde{S}(p, r)$ be the function that does not depend on p . Then, for each i ,

$$S(p_i, r_i) - S(q_i, r_i) = \left[\tilde{S}(p_i, r_i) + d(r_i)\right] - \left[\tilde{S}(q_i, r_i) - d(r_i)\right] = \tilde{S}(p_i, r_i) - \tilde{S}(q_i, r_i). \quad (39)$$

Combining (38) and (39) gives us the result.

B.2 Proof of Theorem 2

The proof closely resembles the proof of Theorem 4 in Howard et al. (2021). Fix $c = 1$ without loss of generality, so that $\hat{\delta}_i$, δ_i , and γ_i are each bounded by $[-\frac{1}{2}, \frac{1}{2}]$ and consequently the differences $\hat{\delta}_i - \delta_i$ and $\hat{\delta}_i - \gamma_i$ are bounded by $[-1, 1]$.

Our goal is to show that

$$L_t(\lambda) = \exp \left\{ \lambda S_t - \psi_E(\lambda) \sum_{i=1}^t (\hat{\delta}_i - \gamma_i)^2 \right\} \quad (40)$$

is a supermartingale for each $\lambda \in [0, 1]$, where $\psi_E(\lambda) = \psi_{E,1}(\lambda) = -\log(1 - \lambda) - \lambda$.

Let $Y_i = \hat{\delta}_i - \delta_i$ and $Z_i = \gamma_i - \delta_i$, such that $Y_i - Z_i = \hat{\delta}_i - \gamma_i \in [-1, 1]$. Using the fact that $\exp \{ \lambda \xi - \psi_E(\lambda) \xi^2 \} \leq 1 + \lambda \xi$ for all $\lambda \in [0, 1]$ and $\xi \geq -1$ (Fan et al., 2015), we have

$$\exp \left\{ \lambda (Y_i - Z_i) - \psi_E(\lambda) (Y_i - Z_i)^2 \right\} \leq 1 + \lambda (Y_i - Z_i).$$

Multiplying each side by $e^{\lambda Z_i}$, we get

$$\exp \left\{ \lambda Y_i - \psi_E(\lambda) (Y_i - Z_i)^2 \right\} \leq e^{\lambda Z_i} (1 - \lambda Z_i) + \lambda e^{\lambda Z_i} Y_i.$$

Now, conditional on \mathcal{G}_{i-1} , we know that $\mathbb{E}[Y_i | \mathcal{G}_{i-1}] = \mathbb{E}[\hat{\delta}_i - \delta_i | \mathcal{G}_{i-1}] = 0$ by the first condition. We also know that $(Z_i)_{i=1}^\infty$ is predictable w.r.t. $(\mathcal{G}_i)_{i=1}^\infty$, as $(\gamma_i)_{i=1}^\infty$, $(p_i)_{i=1}^\infty$, $(q_i)_{i=1}^\infty$, $(r_i)_{i=1}^\infty$ are all predictable w.r.t. $(\mathcal{G}_i)_{i=1}^\infty$. Thus, by taking conditional expectations on both sides, and substituting back $Y_i = \hat{\delta}_i - \delta_i$ and $Z_i = \gamma_i - \delta_i$ on the left-hand side, we get

$$\begin{aligned} \mathbb{E} \left[\exp \left\{ \lambda (\hat{\delta}_i - \delta_i) - \psi_E(\lambda) (\hat{\delta}_i - \gamma_i)^2 \right\} \middle| \mathcal{G}_{i-1} \right] &\leq e^{\lambda Z_i} (1 - \lambda Z_i) + \lambda e^{\lambda Z_i} \mathbb{E}[Y_i | \mathcal{G}_{i-1}] \\ &= e^{\lambda Z_i} (1 - \lambda Z_i) \leq 1, \end{aligned}$$

using $1 - x \leq e^{-x}$ for the final inequality.

Finally, observe that the left-hand side is precisely the expected increment of $(L_t(\lambda))_{t=1}^\infty$ at time t . It follows that $\mathbb{E}[L_t(\lambda) | \mathcal{G}_{t-1}] \leq L_{t-1}(\lambda)$, i.e., $(L_t(\lambda))_{t=1}^\infty$ is a supermartingale. Thus, by (36) and (37), we have

$$\mathbb{P} \left(\exists t \geq 1 : S_t \geq u(\hat{V}_t) \right) \leq \alpha \quad (41)$$

for a sub- ψ_E (i.e., sub-exponential) uniform boundary u with crossing probability $\alpha/2$ and scale $c = 1$. Using the fact that $\frac{1}{t} S_t = \frac{1}{t} \sum_{i=1}^t \hat{\delta}_i - \frac{1}{t} \sum_{i=1}^t \delta_i = \hat{\Delta}_t - \Delta_t$, we can divide each side of the inequality by t to obtain the upper confidence bound. Finally, by applying the same argument to $(-S_t, \hat{V}_t)$ and combining the upper and lower bounds with a union bound, we obtain the CS:

$$\mathbb{P} \left(\forall t \geq 1 : \left| \hat{\Delta}_t - \Delta_t \right| < \frac{u(\hat{V}_t)}{t} \right) \geq 1 - \alpha. \quad (42)$$

B.3 Proof of Theorem 3

Let $S_t = \sum_{i=1}^t (\hat{\delta}_i - \delta_i) = t(\hat{\Delta}_t - \Delta_t)$ and $\hat{V}_t = \sum_{i=1}^t (\hat{\delta}_i - \gamma_i)^2$ where $(\gamma_i)_{i=1}^\infty$ is predictable w.r.t. $(\mathcal{G}_i)_{i=1}^\infty$. As shown in the proof of Theorem 2 (Appendix B.2), we have that, for any $\lambda \in [0, \lambda_{\max}]$,

$$L_t(\lambda) := \exp \left\{ \lambda S_t - \psi_E(\lambda) \hat{V}_t \right\} \quad (43)$$

is a supermartingale w.r.t. $(\mathcal{G}_t)_{t=1}^\infty$, that is, $\mathbb{E}[L_t(\lambda) | \mathcal{G}_{t-1}] \leq L_{t-1}(\lambda)$ for each t .

Now, under $H_0^w(p, q)$, we have that $\exp\{-\lambda \sum_{i=1}^t \delta_i\} \geq 1$, so

$$\begin{aligned} L_t(\lambda) &= \exp\left\{\lambda \sum_{i=1}^t \hat{\delta}_i - \psi_E(\lambda) \hat{V}_t\right\} \exp\left\{-\lambda \sum_{i=1}^t \delta_i\right\} \\ &\geq \exp\left\{\lambda \sum_{i=1}^t \hat{\delta}_i - \psi_E(\lambda) \hat{V}_t\right\} = E_t(\lambda). \end{aligned} \quad (44)$$

Note that $(E_t(\lambda))_{t=1}^\infty$ is adapted to $(\mathcal{G}_t)_{t=1}^\infty$. Because $L_t(\lambda)$ is a supermartingale w.r.t. $(\mathcal{G}_t)_{t=1}^\infty$, it then follows that, under H_0^w , at any stopping time τ ,

$$\mathbb{E}[E_\tau(\lambda)] \leq \mathbb{E}[L_\tau(\lambda)] \leq 1 \quad (45)$$

where the last inequality follows from Doob's optional stopping theorem (Doob, 1940) and that $L_0(\lambda) = 1$ vacuously.

B.4 Proof of Lemma 3

Let \tilde{S} be a linear equivalent of S . Define $\tilde{S}_{\mathbf{w}}$ as follows:

$$\tilde{S}_{\mathbf{w}}(\mathbf{p}_t, r_t) := \sum_{k=1}^K w_k \tilde{S}(p_t^{(k)}, r_t). \quad (46)$$

Then, $\tilde{S}_{\mathbf{w}}$ is a linear equivalent of $S_{\mathbf{w}}$, as for any \mathbf{p} and r , $\tilde{S}(\mathbf{p}, r)$ is a linear function of r and $S(\mathbf{p}, r) - \tilde{S}(\mathbf{p}, r) = \sum_{k=1}^K w_k [S(p^{(k)}, r) - \tilde{S}(q^{(k)}, r)]$ does not depend on \mathbf{p} .

We now show the analogs of (38) and (39) using the linearity of sums in $S_{\mathbf{w}}$ and $\tilde{S}_{\mathbf{w}}$. First note that, because $p_t^{(k)}$ is a forecast made at the beginning of round $t - k + 1$, it only uses information available to forecasters up to time $t - k$, i.e., $p_t^{(k)} \in \mathcal{F}_{t-k}$. (For example, $p_t^{(1)} \in \mathcal{F}_{t-1}$, i.e., 1-step ahead forecasts are predictable w.r.t. $(\mathcal{F}_t)_{t=1}^\infty$, consistent with our previous formulation in Section 3.2.) It then follows that $(p_t^{(k)})_{t=1}^\infty$ is predictable w.r.t. $(\mathcal{F}_t)_{t=1}^\infty$ and $(\mathcal{G}_t)_{t=1}^\infty$ for each k , as $p_t^{(k)} \in \mathcal{F}_{t-k} \subseteq \mathcal{F}_{t-1} \subsetneq \mathcal{G}_{t-1}$. This gives us the analog of (38):

$$\mathbb{E} \left[\tilde{S}_{\mathbf{w}}(\mathbf{p}_t, y_t) \mid \mathcal{G}_{t-1} \right] = \sum_{k=1}^K w_k \mathbb{E} \left[\tilde{S}(p_t^{(k)}, y_t) \mid \mathcal{G}_{t-1} \right] = \sum_{k=1}^K w_k \tilde{S}(p_t^{(k)}, r_t) = \tilde{S}_{\mathbf{w}}(\mathbf{p}_t, r_t). \quad (47)$$

Also, analogous to (39), we have that

$$\begin{aligned} S_{\mathbf{w}}(\mathbf{p}_t, r_t) - S_{\mathbf{w}}(\mathbf{q}_t, r_t) &= \sum_{k=1}^K w_k [S(p_t^{(k)}, r_t) - \tilde{S}(q_t^{(k)}, r_t)] \\ &= \sum_{k=1}^K w_k \left[(\tilde{S}(p_t^{(k)}, r_t) + d(r_t)) - (\tilde{S}(q_t^{(k)}, r_t) - d(r_t)) \right] \\ &= \sum_{k=1}^K w_k [\tilde{S}(p_t^{(k)}, r_t) - \tilde{S}(q_t^{(k)}, r_t)] \\ &= \tilde{S}_{\mathbf{w}}(\mathbf{p}_t, r_t) - \tilde{S}_{\mathbf{w}}(\mathbf{q}_t, r_t) \end{aligned} \quad (48)$$

where $d(r) := S(p, r) - \tilde{S}(p, r)$ is the function that does not depend on p .

Given (47) and (48), the proof of Theorem 2 can readily be extended to derive the analogous confidence sequences for average forecast score differentials under $S_{\mathbf{w}}$. We state this extension as a corollary.

B.5 Proof of Lemma 4

First, observe that $(T(p_t, q_t))_{t=1}^\infty$ is predictable w.r.t. $(\mathcal{G}_t)_{t=1}^\infty$, since $T(p_t, q_t) \in \mathcal{F}_{t-1} \subset \mathcal{G}_{t-1}$. This means that the equivalent of (38) holds for (32):

$$\begin{aligned}\mathbb{E}[w(p_t, q_t, y_t) \mid \mathcal{G}_{t-1}] &= \frac{\mathbb{E}[S(p_t, y_t) - S(q_t, y_t) \mid \mathcal{G}_{t-1}]}{T(p_t, q_t)} \\ &= \frac{\mathbb{E}[\tilde{S}(p_t, y_t) - \tilde{S}(q_t, y_t) \mid \mathcal{G}_{t-1}]}{T(p_t, q_t)} \\ &= \frac{\tilde{S}(p_t, r_t) - \tilde{S}(q_t, r_t)}{T(p_t, q_t)} \\ &= \frac{S(p_t, r_t) - S(q_t, r_t)}{T(p_t, q_t)} = w(p_t, q_t, r_t),\end{aligned}$$

where we use (39) in the second and fourth equalities and (38) in the third equality. Note that the score differences are bounded by a value that depends on both q_0 and S . For the Brier score, this bound is given by $[-\frac{2}{q_0}, \frac{2}{q_0}]$.

C Computing the Gamma-Exponential Mixture

Here, we derive the gamma-exponential mixture corresponding to the e-process for the weak null, as discussed in Section 3.5. By Proposition 9 in Howard et al. (2021), the expression for the gamma-exponential mixture is given by

$$m(s, v) := \frac{\left(\frac{\rho}{c^2}\right)^{\frac{\rho}{c^2}}}{\Gamma\left(\frac{\rho}{c^2}\right) P\left(\frac{\rho}{c^2}, \frac{\rho}{c^2}\right)} \frac{\Gamma\left(\frac{v+\rho}{c^2}\right) P\left(\frac{v+\rho}{c^2}, \frac{cs+v+\rho}{c^2}\right)}{\left(\frac{cs+v+\rho}{c^2}\right)^{\frac{v+\rho}{c^2}}} \exp\left\{\frac{cs+v}{c^2}\right\}, \quad (49)$$

where $\Gamma(a, z) := \int_z^\infty u^{a-1} e^{-u} du$ is the upper incomplete gamma function, $\Gamma(a) := \Gamma(a, 0)$ is the gamma function, and P is the regularized lower incomplete gamma function defined as

$$P(a, z) := \frac{1}{\Gamma(a)} \int_0^z u^{a-1} e^{-u} du \quad (50)$$

for $a, z > 0$. Note that both Γ and P can be computed efficiently in standard scientific computing software. (E.g., P can be computed using `boost::math::gamma_p` in C++ and `scipy.special.gammainc` in Python.)

In the following, we derive the expression (49) and show its upper bound in the case where $s + v + \rho < 0$. For notational simplicity, we assume $c = 1$, but an analogous proof can be made for any $c > 0$.

Recall that $\psi_E(\lambda) = -\log(1 - \lambda) - \lambda$ for $\lambda \in [0, 1]$. Using the gamma density $f_\rho(\lambda) =$

$C(\rho)(1 - \lambda)^{\rho-1}e^{-\rho(1-\lambda)}$, where $C(\rho) = \frac{\rho^\rho}{P(\rho, \rho)\Gamma(\rho)}$, we have that, for $\rho > 0$,

$$\begin{aligned}
m(s, v) &= C(\rho) \int_0^1 \exp \{ \lambda s - \psi_E(\lambda)v \} \cdot (1 - \lambda)^{\rho-1}e^{-\rho(1-\lambda)} d\lambda \\
&= C(\rho) \int_0^1 e^{\lambda(s+v)}(1 - \lambda)^v \cdot (1 - \lambda)^{\rho-1}e^{-\rho(1-\lambda)} d\lambda \\
&= C(\rho) \int_0^1 (1 - \lambda)^{v+\rho-1}e^{\lambda(s+v)-\rho(1-\lambda)} d\lambda \\
&= C(\rho) \left(\int_0^1 (1 - \lambda)^{v+\rho-1}e^{-(s+v+\rho)(1-\lambda)} d\lambda \right) e^{s+v},
\end{aligned} \tag{51}$$

where in the last equality we used

$$\lambda(s + v) - \rho(1 - \lambda) = (s + v) - (1 - \lambda)(s + v) - (1 - \lambda)\rho = -(s + v + \rho)(1 - \lambda) + (s + v).$$

Now, let $a = v + \rho$ and $z = s + v + \rho$, and note that $a > 0$.

If $z > 0$, then using the change-of-variable formula $u = (s + v + \rho)(1 - \lambda) = z(1 - \lambda)$, we have that

$$\begin{aligned}
m(s, v) &= C(\rho) \left(\int_z^0 \left(\frac{u}{z} \right)^{a-1} e^{-u} \frac{du}{-z} \right) e^{s+v} \\
&= C(\rho) \cdot \frac{1}{z^a} \left(\int_0^z u^{a-1} e^{-u} du \right) e^{s+v}
\end{aligned} \tag{52}$$

$$= C(\rho) \frac{\Gamma(a)P(a, z)}{z^a} e^{s+v}, \tag{53}$$

where we use the fact that the integral in (52) corresponds to the numerator of the lower incomplete gamma function $P(a, z)$ in (50). The expression (53) can be computed in closed-form.

On the other hand, if $z < 0$, then using the change-of-variable formula $u = -(s + v + \rho)(1 - \lambda) = -z(1 - \lambda)$, we obtain

$$\begin{aligned}
m(s, v) &= C(\rho) \left(\int_{-z}^0 \left(\frac{u}{-z} \right)^{a-1} e^u \frac{du}{z} \right) e^{s+v} \\
&= C(\rho) \cdot \frac{1}{(-z)^a} \left(\int_0^{-z} u^{a-1} e^u du \right) e^{s+v} \\
&= C(\rho) \cdot \frac{1}{|z|^a} \left(\int_0^{|z|} u^{a-1} e^u du \right) e^{s+v}.
\end{aligned} \tag{54}$$

Although the integral in (54) is no longer a regularized lower gamma function, we can still

show that $m(s, v)$ as a whole is bounded by e . Since $e^u \leq e^{|z|} = e^{-z}$ for $u \leq |z|$, we have that

$$\begin{aligned} m(s, v) &\leq C(\rho) \cdot \frac{1}{|z|^a} \left(\int_0^{|z|} u^{a-1} du \right) e^{-z} \cdot e^{s+v} \\ &= C(\rho) \cdot \frac{1}{|z|^a} \left(\int_0^{|z|} u^{a-1} du \right) e^{-\rho} \end{aligned} \quad (55)$$

$$\begin{aligned} &= C(\rho) \cdot \frac{1}{|z|^a} \left(\frac{u^a}{a} \right) \Big|_0^{|z|} e^{-\rho} \\ &= \frac{C(\rho)e^{-\rho}}{v + \rho}, \end{aligned} \quad (56)$$

where in (55) we used $-z + (s + v) = -(s + v + \rho) + (s + v) = -\rho$, and in (56) we substituted in $a = v + \rho$. We can further bound this value, using the fact that $v > 0$ and substituting back in $C(\rho)$:

$$\begin{aligned} m(s, v) &\leq \frac{C(\rho)e^{-\rho}}{v + \rho} \leq \frac{C(\rho)e^{-\rho}}{\rho} \\ &= \rho^{\rho-1} e^{-\rho} \cdot \left(\int_0^\rho u^{\rho-1} e^{-u} du \right)^{-1} \\ &\leq \rho^{\rho-1} e^{-\rho} \cdot \left(e^{-\rho} \int_0^\rho u^{\rho-1} du \right)^{-1} \end{aligned} \quad (57)$$

$$\begin{aligned} &= \rho^{\rho-1} \cdot \left[\left(\frac{u^\rho}{\rho} \right) \Big|_0^\rho \right]^{-1} \\ &= 1, \end{aligned} \quad (58)$$

where in (57) we used the fact that $e^{-\rho} \leq e^{-u}$ for $u \in [0, \rho]$. It makes sense that $m(s, v)$ is upper-bounded by 1 when $z = s + v + \rho < 0$, because $s < -(v + \rho) < 0$ would imply that the sum of score differentials is negative, which is an evidence that supports the weak null. In our implementation, we use the upper bound (56), which can be computed easily and gets substantially smaller than 1 when $v + \rho \gg 0$.

D Comparing CS Widths on IID Means

To validate and finetune our CSs, we compare the widths of various time-uniform CS applicable to the mean of independent and identically distributed (IID) random variables. We compare both the Hoeffding-style (H) CS (Theorem 1) and the empirical-Bernstein (EB) CS (Theorem 2) using both the conjugate-mixture (CM) and the polynomial stitching uniform boundaries, as described in Section 3.4. We also include predictable-mixed confidence sequences, namely the predictably-mixed Hoeffding (PM-H) CS and empirical Bernstein (PM-EB) CS from [Waudby-Smith and Ramdas \(2020\)](#), which are time-uniform CS that are also applicable for means of IID random variables. We also include the asymptotic CS described in [Waudby-Smith et al. \(2021\)](#). As for the data, we use the difference between two i.i.d. Beta random variables, as a proxy for score differentials between two sets of forecasts: for $i = 1, \dots, 10,000$,

$$\delta_i \stackrel{\text{IID}}{\sim} \text{Beta}(30, 10) - \text{Beta}(10, 30). \quad (59)$$

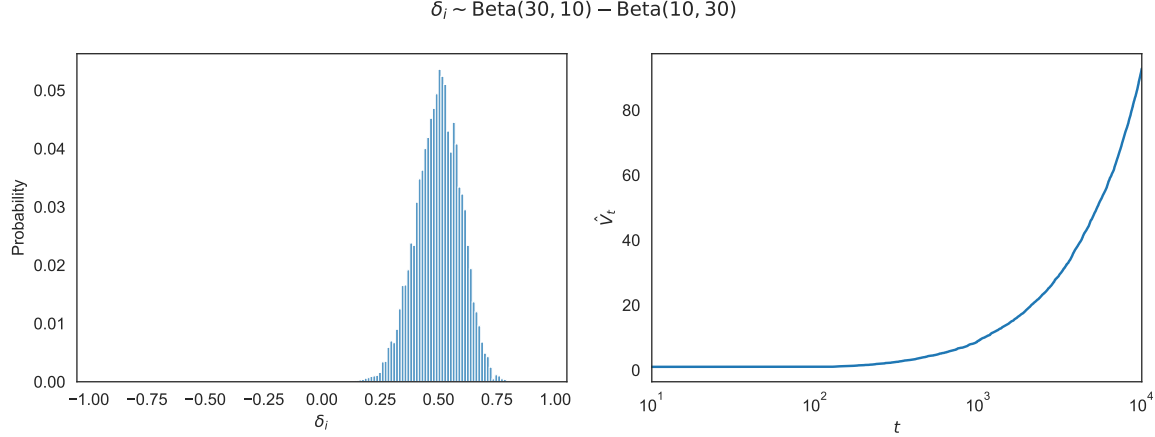


Figure 10: (Left) Histogram of $\delta_i \stackrel{\text{IID}}{\sim} \text{Beta}(30, 10) - \text{Beta}(10, 30)$ for $i = 1, \dots, 10,000$. (Right) Plot of the intrinsic time $\hat{V}_t = \sum_{i=1}^t (\hat{\delta}_i - \hat{\Delta}_{i-1})^2$, where $\hat{\Delta}_{i-1} = \sum_{j=1}^{i-1} \hat{\delta}_j$. Note that the horizontal axis t is drawn in log-scale. Also note that the hyperparameter v_{opt} determines the intrinsic time \hat{V}_t at which the uniform boundary is the tightest.

Note that $-1 \leq \delta_i \leq 1$ a.s. and that $\mathbb{E}[\delta_i] = \frac{30}{30+10} - \frac{10}{10+30} = \frac{1}{2}$. Figure 10 illustrates the data sampled according to (59) (left) as well as the intrinsic time $\hat{V}_t = \sum_{i=1}^t (\hat{\delta}_i - \hat{\Delta}_{i-1})^2$, where $\hat{\Delta}_{i-1} = \sum_{j=1}^{i-1} \hat{\delta}_j$, over time (right). Note that, when choosing the uniform boundary for the CSs, the hyperparameter v_{opt} determines the intrinsic time \hat{V}_t at which the width of the uniform boundary is the tightest (Proposition 3, [Howard et al. \(2021\)](#)).

In Figure 11 (left), we present the hyperparameter tuning results of the CM-EB CS with respect to its optimal intrinsic time parameter v_{opt} , which corresponds to the point in the variance process where the boundary is the tightest. As a point of comparison, we also plot the polynomial stitching EB CS with hyperparameters $v_{\text{opt}} = 10$, $s = 1.4$, and $\eta = 2$. Comparing the values of $v_{\text{opt}} \in \{0.1, 1, 10, 100, 1000\}$, we find that the CM-EB CS is the tightest across time (up to $T = 10^4$) with $v_{\text{opt}} = 10$. Based on these results, we use the CM-EB CS with $v_{\text{opt}} = 10$ for our other experiments throughout the paper (except for the baseball experiments, which we conduct as a post-hoc analysis using the sample variance from the data).

In Figure 11 (right), we plot the widths of the different kinds of time-uniform CS, optimized for the intrinsic time $v_{\text{opt}} = 10$ when applicable. Generally speaking, we observe that the CSs are the tightest for the asymptotic CS, followed by the EB CS variants and the Hoeffding CS variants. This is consistent with our intuition, as the EB CS additionally makes use of the estimated variance to achieve smaller widths than the Hoeffding CS, and the asymptotic CS is the “limit” of EB CS in terms of the width while sacrificing the non-asymptotic guarantee ([Waudby-Smith et al., 2021](#)). For the EB CS variants, the CM-EB CS is tighter towards the beginning ($t < 10^3$) while the PM-EB CS becomes slightly tighter afterwards, and the stitching CS is not as tight as the other two. This is also as expected, as the CM-EB and PM-EB CS have similar widths (up to differences determined by the choice of hyperparameters) ([Waudby-Smith and Ramdas, 2020](#)) and the stitching CS tends to be looser in practice ([Howard et al., 2021](#)). This trend is also analogous for the Hoeffding CS variants, although the stitching variant does become tighter for larger t in this case.

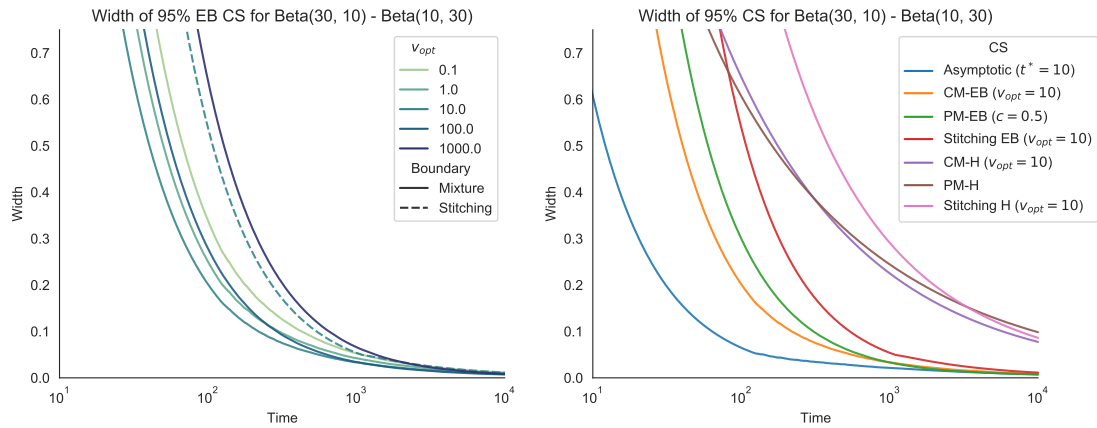


Figure 11: (Left) Hyperparameter tuning for the width of CM-EB CS by adjusting the optimal intrinsic time parameter v_{opt} . The choice $v_{opt} = 10$ gives the smallest width overall, although $v_{opt} = 100$ is comparable for $t > 10^3$. The width of stitching EB CS (with $v_{opt} = 1$) is also drawn as a point of comparison. (Right) Comparing the widths of different types of time-uniform CS. Overall, the asymptotic CS is the tightest, followed by the EB variants and then by the Hoeffding variants.